Theory of charge transport in a quantum dot tunnel junction with multiple energy levels

Yia-Chung Chang*
Research Center for Applied Sciences, Academia Sinica, Taipei 115, Taiwan
and Department of Physics, University of Illinois at Urbana-Champaign, Urbana, Illinois 61801, USA

David M.-T. Kuo†
Department of Electrical Engineering, National Central University, Chung-Li 320, Taiwan
(Received 12 February 2008; revised manuscript received 16 April 2008; published 9 June 2008)

Transport properties of nanoscale quantum dots embedded in a matrix connected with metallic electrodes are investigated theoretically. The Green's function method is used to calculate the tunneling current of an Anderson model with multiple energy levels, which is employed to model the nanoscale tunnel junction of concern. A closed form spectral function of a quantum dot or coupled dots (with arbitrary number of energy levels) embedded in a tunnel junction is derived and rigorously proved via the principle of induction. Such an expression can give an efficient and reliable way for analyzing the complicated current spectra of a quantum dot tunnel junction. Besides, it can also be applied to the coupled dots case, where the negative differential conductance due to the proximity effect is found. Finally, we investigate the case of bipolar tunneling, in which both electrons and holes are allowed to tunnel into the quantum dot, while optical emission occurs. We find dramatic changes in the emission spectra as the applied bias is varied.

DOI: 10.1103/PhysRevB.77.245412 PACS number(s): 73.63.Kv, 73.21.La, 73.63.Rt, 73.61.Ga

I. INTRODUCTION

Recently, nanoscale quantum dots (so-called artificial atoms or molecules) have been extensively studied for their potential applications in novel nanostructure devices based on the quantum tunneling process. Such quantum dot tunneling devices include electrically driven single-photon emitters,[1,2] single-electron transistors (SETs),[3,4] and solid state quantum bits.[5] Proposals have been made to integrate these tunneling devices into circuits and apply them as biosensors to detect the DNA sequence.[6] For such applications, it is very important to have good control of the current-voltage characteristics (CVC) of these devices. The CVC of tunneling devices depend not only on the material of the quantum dot but also on its shape, size, and location. Interesting physical phenomena of such devices, including bistable current,[7] negative differential conductance,[8] Fano resonance, and Kondo effect[9] have been extensively investigated. However, most of these studies focus on the properties of the ground state only (one level) rather than multiple levels. In realistic nanojunction devices, the consideration of multiple energy levels is essential in order to understand fully their CVC and the effects due to interaction with neighboring quantum dots and charged defects in the local environment.

Theoretical calculations based on the tight-binding,[10] pseudopotential,[11] $k\cdot p$,[12] or bond-orbital method[13] can provide the energy level separations and charging energies of quantum dots. However, these calculations require the knowledge of shape and size of the quantum dot, which is usually difficult to obtain experimentally, since the quantum dots are typically embedded in a matrix in most tunneling devices. Apart from that, the tunneling rates arising from the coupling between the quantum dots and electrodes as well as the electron Coulomb interactions also significantly influence the CVC of these tunneling devices.[8] Consequently, it is difficult to model the *I-V* curves of devices via *ab initio* methods.[14,15]

Although the energy level separations and charging energies of individual quantum dots have been reported in many SET experiments,[3,4] both of these physical quantities of SETs were only qualitatively estimated due to the unknown junction capacitances (which are related to the location of individual quantum dots between electrodes and the geometry of quantum dots). Recently, tunneling current spectra of an STM-tip and/or quantum dot tunnel structure have been studied experimentally.[16–22] Because the shell-filling and shell-tunneling conditions of a quantum dot significantly influence the probability for resonant tunneling through each individual energy level, it is difficult to identify the origin of the peaks observed in tunneling current spectra without a reliable theoretical guidance.[16–22] To analyze the complicated tunneling spectra in these measurements, it is desirable to have a simple yet reliable formula that allows one to determine the CVC characteristics associated with the multiple energy levels involved and the interplay of the intralevel and interlevel Coulomb interactions.

We have employed the Anderson model with arbitrary energy levels to describe the strongly correlated system, as shown in Fig. 1. The tunneling current through the quantum dots can be obtained via the nonequilibrium Green's function method.[9,23,24] Such a method has been extensively used to investigate the Coulomb blockade and the Kondo effect on the tunneling current through the ground state of a single quantum dot.[9,25] In a previous article,[8] we reported a closed form expression for the spectral function, which can be used to reveal the current spectra of not only a single dot but also coupled quantum dots. We found that specific evaluation of both the two-particle occupation number as well as the single-particle occupation number is important for determining the probability of each resonant-tunneling channel. In the present paper, we provide a more detailed description of the above study and give a mathematically rigorous proof to the formulas derived via the principle of induction. Furthermore, we investigate the case of bipolar tunneling, in which both

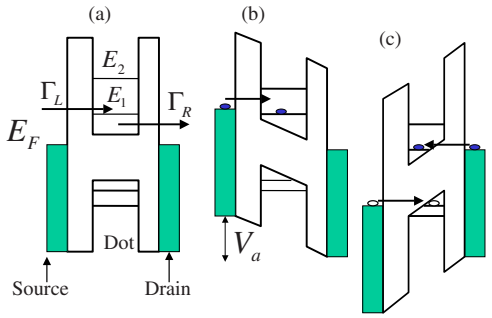

FIG. 1. (Color online) Schematic energy diagram for a quantum dot junction of concern. Γ_L and Γ_R denote, respectively, the tunneling rates for electrons from the source to the quantum dot and from the quantum dot to the drain (which is grounded). (a) System without bias and (b) System with forward bias. (c) System with reverse bias.

electrons and holes are allowed to tunnel into the quantum dot, while optical emission occurs. We also calculate the consequent optical emission due to the bipolar tunneling and we find that dramatic changes in the emission spectra occur as the applied bias is varied.

II. ELECTRON TUNNELING CURRENT

We start with the following Hamiltonian for describing the system of a metal/quantum dot (nanostructure)/metal double barrier junction, as shown in Fig. 1:

$$H = \sum_{k,\sigma,\beta} \epsilon_k a^\dagger_{k,\sigma,\beta} a_{k,\sigma,\beta} + \sum_{\ell,\sigma} E_\ell d^\dagger_{\ell,\sigma} d_{\ell,\sigma} + \frac{1}{2} \sum_{\ell,j,\sigma,\sigma'} U_{\ell,j} d^\dagger_{\ell,\sigma} d_{\ell,\sigma} d^\dagger_{j,\sigma'} d_{j,\sigma'} + \sum_{k,\sigma,\beta,\ell} V_{k,\beta,\ell} a^\dagger_{k,\sigma,\beta} d_{\ell,\sigma} + \sum_{k,\sigma,\beta,\ell} V^*_{k,\beta,\ell} d^\dagger_{\ell,\sigma} a_{k,\sigma,\beta}, \quad (1)$$

where $a^\dagger_{k,\sigma,\beta}$ ($a_{k,\sigma,\beta}$) creates (annihilates) an electron of momentum k and spin σ with energy ϵ_k in the β metallic electrode. $d^\dagger_{\ell,\sigma}$ ($d_{\ell,\sigma}$) creates (annihilates) an electron inside the quantum dot with orbital energy E_ℓ, $U_{\ell,j}$ describes the on-site interlevel Coulomb energy between levels ℓ and j, and $V_{k,\beta,\ell}$ describes the coupling between the band states of electrodes and quantum dot states. The Hamiltonian given by Eq. (1) is based on the Anderson model with multiple energy levels.[9,26]

The tunneling current can be expressed as[23]

$$J = \frac{-2e}{\hbar} \sum_\ell \int \frac{d\epsilon}{2\pi} [f_L(\epsilon - \mu_L) - f_R(\epsilon - \mu_R)] \times \frac{\Gamma_{\ell,L}(\epsilon)\Gamma_{\ell,R}(\epsilon)}{\Gamma_{\ell,L}(\epsilon) + \Gamma_{\ell,R}(\epsilon)} \mathrm{Im}\, G^r_{\ell,\sigma}(\epsilon), \quad (2)$$

where $f_L(\epsilon)$ and $f_R(\epsilon)$ are the Fermi distribution functions for the left and right electrodes (source and drain), respectively. The chemical potential difference between these two electrodes is related to the applied bias, $\mu_L - \mu_R = eV_a$. $\Gamma_{\ell,L}(\epsilon)$ and $\Gamma_{\ell,R}(\epsilon)[\Gamma_{\ell,\beta} = 2\pi\Sigma_{\mathbf{k}}|V_{\ell,\beta,\mathbf{k}}|^2 \delta(\epsilon - \epsilon_{\mathbf{k}})]$ denote the tunneling rates from the quantum dot to the left and right electrodes, respectively. The notations e and $\hbar$ denote the electron charge and Plank's constant. The expression of Eq. (2) is nothing but the Landauer formula,[27] which is valid even though on-site Coulomb interactions are taken into account. The detailed derivation of Eq. (2) is similar to that of Ref. 28. For simplicity, these tunneling rates will be assumed to be energy and bias independent. Note that the tunneling rates can be calculated numerically.[29] Therefore, the calculation of tunneling current is entirely determined by the spectral function of $A = \mathrm{Im}\, G^r_{\ell,\sigma}(\epsilon)$, which is the imaginary part of the retarded Green's function $G^r_{\ell,\sigma}(\epsilon)$.

The expression of retarded Green's function $G^r_{\ell,\sigma}(\epsilon)$ can be obtained by solving the equation of motion for $G^r_{\ell,\sigma}(t) = -i\theta(t)\langle\{d_{\ell,\sigma}(t), d^\dagger_{\ell,\sigma}(0)\}\rangle$, where $\theta(t)$ is a step function, the curly brackets denote the anticommutator, and the angular bracket $\langle\cdots\rangle$ means "thermal average." The equation of motion method has been used to investigate charge transport through the Anderson model.[30,31] In Ref. 30, the differential conductance of electron transport through quantum dot with multiple levels and a constant Coulomb interaction was investigated based on the linear-response theory. Their treatment corresponds to Beenakker's approach, which calculates the distribution function of N electrons in a quantum dot using the detailed balance equations.[32] Here, we derive the spectral function for a QD tunnel junction with arbitrary number of energy levels by solving the equations of motion directly.

The Fourier transform of $G^r_{\ell,\sigma}(t)$ is given by

$$G^r_{\ell,\sigma}(\epsilon) = \int_{-\infty}^{\infty} dt G^r_{\ell,\sigma}(t) e^{i(\epsilon + i\eta)t}, \quad (3)$$

with η as a positive infinitesimal number. After some tedious algebraic operations, rigorous solution to $G^r_{\ell,\sigma}(\epsilon)$ in the Coulomb blockade regime can be obtained by solving a hierarchy of equations of motion, relating $G^r_{\ell,\sigma}$ to two-particle Green's functions, $G^r_{\ell,\ell}(\epsilon)$, which in turn is related recursively upward to the $2M$-particle Green's function, $G^r_{2M}(\epsilon)$. For the fully occupied configuration, the corresponding Green's function $G^r_{2M}(\epsilon)$ can be solved immediately due to the self-termination of the hierarchy of equations of motion, since a fully occupied configuration can no longer be linked to a different configuration with more particles. By keeping the two-particle correlation functions associate with the same level, we can obtain neat closed form expressions for all Green's functions involved. The detailed derivations (which are proved rigorously via the principle of induction) are given in Appendixes A and B. We obtain

$$G^r_{2M} = \frac{N_{\ell,-\sigma} \prod'_j c_j}{(\mu_l - U_\ell - 2\sum'_j U_{\ell,j})}, \quad (4)$$

where $\mu_\ell \equiv \epsilon - E_\ell + i(\Gamma_{\ell,L} + \Gamma_{\ell,R})/2$ and U_ℓ denotes the intralevel Coulomb energy in level ℓ. $N_{j,-\sigma} = \langle n_{j,-\sigma}\rangle$ and $c_j = \langle n_{j,-\sigma} n_{j,\sigma}\rangle$ denote the one-particle and two-particle average occupancies in the level j. Here and henceforth, Π'_j means

taking the product of terms labeled by j with $j=1\cdots M$, excluding ℓ.

$$G^r_{\ell,\ell}(\epsilon) = \prod_j{}' (\hat{a}_j + \hat{b}_j + c_j) G^r_{2M} / \prod_j{}' c_j \equiv N_{\ell,-\sigma} \sum_{m=1}^{3^{M-1}} \frac{p_m}{\mu_\ell - U_\ell - \Pi_m}, \quad (5)$$

and

$$G^r_{\ell,\sigma}(\epsilon) = (\hat{b}_\ell N^{-1}_{\ell,-\sigma} + 1) G^r_{\ell,\ell}(\epsilon) = (1 - N_{\ell,-\sigma}) \sum_{m=1}^{3^{M-1}} \frac{p_m}{\mu_\ell - \Pi_m} + N_{\ell,-\sigma} \sum_{m=1}^{3^{M-1}} \frac{p_m}{\mu_\ell - U_\ell - \Pi_m}, \quad (6)$$

where $\hat{b}_\ell$, $\hat{a}_j$, and $\hat{b}_j$ are the operators that put a factor $b_\ell = 1 - N_{\ell,-\sigma}$, $a_j \equiv 1 - (N_{j,\sigma} + N_{j,-\sigma}) + c_j$, and $b_j \equiv N_{j,\sigma} + N_{j,-\sigma} - 2c_j$ in the numerator and increase the value of the denominator by U_ℓ, $2U_{\ell,j}$, and $U_{\ell,j}$, respectively when acting on a fractional function. For example, $\hat{b}_j(f/g) = (b_j f)/(g + U_{\ell,j})$. The operators $\hat{a}_j$ and $\hat{b}_j$, when acting on a term describing the state with two particles in level j, have the physical meanings of removing two particles and one particle, respectively, from that state; thus, converting the state into zero-particle (with probability a_j) and one-particle (with probability b_j) states. Similarly, $\hat{b}_\ell$ has the physical meanings of removing one particle from a state, in which the level ℓ has been occupied by one electron, and converting it into an empty state with probability $b_\ell = 1 - N_{\ell,-\sigma}$. Note that the expression of b_ℓ is different from b_j and the two-particle removing operator $\hat{a}_\ell$ does not exist. This is because level ℓ is the designated level in which the electron transport is considered. Thus, it is not physically meaningful to consider the transport through a state in which the level ℓ is doubly occupied. Consequently, the operator $\hat{b}_\ell$ will only act on a state in which the level ℓ is singly occupied. Namely, level ℓ can be either empty (with probability $1 - N_{\ell,-\sigma}$) or occupied by one electron (with probability N_ℓ) when we consider an electron tunneling through that level.

In the above expressions, Π_m in the denominator denotes the sum of Coulomb interactions seen by a particle in level ℓ due to other particles in configuration m, in which each level $j (j \neq \ell)$ can be occupied by zero, one, or two particles. On the other hand, the numerator p_m denotes the probability of finding the system in configuration m. For a two-level ($M=2$) system ($\ell \neq j$), the two-particle Green's function $G^r_{\ell,\ell}(\epsilon)$ contains three configurations with different occupancies in level j, while always keeping level ℓ occupied with one electron. The three corresponding terms have numerators $p_1 = a_j \equiv 1 - (N_{j,\sigma} + N_{j,-\sigma}) + \langle n_{j,\sigma} n_{j,-\sigma} \rangle$ (the probability with no particle in level j), $p_2 = b_j \equiv N_{j,\sigma} + N_{j,-\sigma} - 2\langle n_{j,\sigma} n_{j,-\sigma} \rangle$ (the probability with one particle in level j), and $p_3 = c_j \equiv \langle n_{j,\sigma} n_{j,-\sigma} \rangle$ (the probability with two particles in level j). Meanwhile, the denominators contain Coulomb energies: $\Pi_1 = 0$, $\Pi_2 = U_{\ell,j}$, and $\Pi_3 = 2U_{\ell,j}$, respectively. For a three-level case ($\ell \neq j \neq j'$), there are nine (3×3) configurations for different occupancies in levels j and j'. The corresponding numerators (probability factors) are given by the expansion of the product $(a_j + b_j + c_j)(a_{j'} + b_{j'} + c_{j'})$. Namely, $p_1 = a_j a_{j'}$, $p_2 = b_j a_{j'}$, $p_3 = a_j b_{j'}$, $p_4 = c_j a_{j'}$, $p_5 = c_{j'} a_j$, $p_6 = b_j b_{j'}$, $p_7 = c_j b_{j'}$, $p_8 = c_{j'} b_j$, and $p_9 = c_j c_{j'}$. The denominators contain the following interlevel Coulomb interaction factors: $\Pi_1 = 0$, $\Pi_2 = U_{\ell,j}$, $\Pi_3 = U_{\ell,j'}$, $\Pi_4 = 2U_{\ell,j}$, $\Pi_5 = 2U_{\ell,j'}$, $\Pi_6 = U_{\ell,j} + U_{\ell,j'}$, $\Pi_7 = 2U_{\ell,j} + U_{\ell,j'}$, $\Pi_8 = 2U_{\ell,j'} + U_{\ell,j}$, and $\Pi_9 = 2U_{\ell,j} + 2U_{\ell,j'}$. Based on these simple rules, the probability factors and interlevel Coulomb interaction factors for any number of energy levels can be similarly determined by applying the product of operators $(\hat{a}_j + \hat{b}_j + c_j)$ on the fully occupied configuration, as described in Eq. (5). It is worth noting that the sum of probability factors p_m for all configurations associated with arbitrary number of levels is always equal to 1, resulting from a sum rule obeyed by $G^r_{\ell,\ell}(\epsilon)$. From Eqs. (4)–(6), we see that the probability of finding the system in each configuration is determined not only by the average one-particle occupancy but also by the average two-particle occupancy. It should be pointed out that for two particles occupying different levels, we still adopt the approximation $\langle n_{\ell,\sigma} n_{j,\sigma'} \rangle \approx N_{\ell,\sigma} N_{j,\sigma'}$, effectively ignoring the correlation of electrons occupying different levels. This is consistent with the Hartree–Fock approximation adopted in the Coulomb blockade regime and it will not lead to unphysical tunneling current as it would otherwise occur had we also assumed $\langle n_{j,\sigma} n_{j,-\sigma} \rangle = N_{j,\sigma} N_{j,-\sigma}$.

$N_{\ell,\sigma}$ and c_ℓ in the above equations can be obtained by solving the following equations self-consistently:

$$N_{\ell,\sigma} = -\int \frac{d\epsilon}{\pi} \frac{\Gamma_{\ell,L} f_L(\epsilon) + \Gamma_{\ell,R} f_R(\epsilon)}{\Gamma_{\ell,L} + \Gamma_{\ell,R}} \mathrm{Im}\, G^r_{\ell,\sigma}(\epsilon), \quad (7)$$

$$c_\ell = -\int \frac{d\epsilon}{\pi} \frac{\Gamma_{\ell,L} f_L(\epsilon) + \Gamma_{\ell,R} f_R(\epsilon)}{\Gamma_{\ell,L} + \Gamma_{\ell,R}} \mathrm{Im}\, G^r_{\ell,\ell}(\epsilon). \quad (8)$$

The values of $N_{\ell,\sigma}$ and c_ℓ are restricted between 0 and 1.

III. UNIPOLAR TUNNELING CURRENT

The fluorescence microscopy and spectroscopy based on cadmium selenite (CdSe) nanoparticles are invaluable analytical tools in biomedical research.[33,34] Consequently, it is important to clarify the electronic structure of a single CdSe QD. We now apply our theory to study electrical transport in a single-electron transistor made of a CdSe QD and metallic leads.[35] Because the electrodes are biased at V_a and V_g, the one-particle energy levels E_ℓ in the CdSe QD are changed to $E_\ell + \alpha_a e V_a + \alpha_g e V_g$. The dimensionless scaling factors α_a and α_g depend on the position and shape of quantum dots and satisfy $\alpha_a \leq 1$ and $\alpha_g \leq 1$. V_g denotes the applied gate voltage just tuning the energy levels of a single dot but not inject any carriers from the gate electrode to the QD. Throughout the paper, the system is assumed at zero temperature. In the forward bias regime, three one-particle energy levels of the CdSe QD are used for modeling the tunneling spectra. The

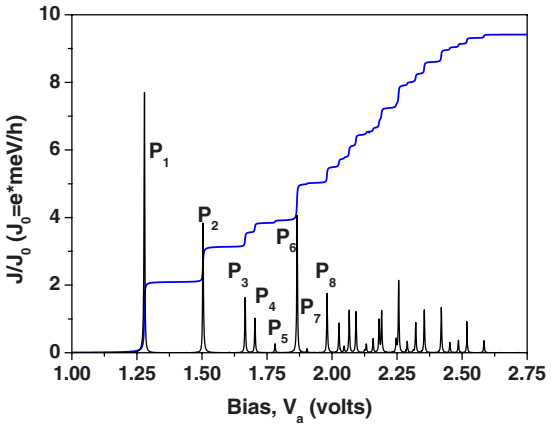

FIG. 2. (Color online) Tunneling current [in the units of $J_0=e\times(\mathrm{meV})/h$] as a function of the applied bias V_a at zero temperature. The relevant parameters are $\alpha=0.61$ and $\Gamma_L=\Gamma_R=1$ meV. The corresponding differential conductance dJ/dV_a is also shown for comparison (the sharp peaks).

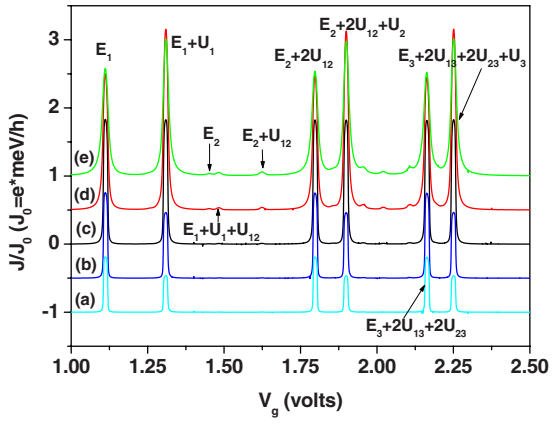

FIG. 3. (Color online) Tunneling current as a function of the gate voltage at $V_a=10$ mV for various ratios of Γ_L/Γ_R: (a) 0.2, (b) 0.4, (c) 1, (d) 5, and (e) 10. Γ_R is fixed at 1 meV.

chemical potentials of both the left electrode and right electrodes are assumed to be 0.78 eV below the ground state energy level E_1 at zero bias. Meanwhile, we choose $E_2-E_1=0.236$ eV, $E_3-E_1=0.456$ eV, $U_1=0.137$ eV, $U_{1,2}=U_{2,1}=0.122$ eV, $U_2=0.07$ eV, $U_3=0.06$ eV, $U_{1,3}=U_{3,1}=0.1$ eV, and $U_{2,3}=U_{3,2}=0.04$ eV. These physical parameters were determined by considering their possible physical range and the best agreement between the calculated and measured tunneling spectra. We note that the p-like level is sixfold degenerate (including spin) due the symmetry of the spherical QD. The coupling strength between the left electrode (or the right electrode) and the p_x- or p_y-like orbital is weak. Therefore, only p_z-like orbital has been included, which is labeled by E_2, while E_3 denotes one of the d-like orbitals that is strongly coupled to the leads.

Occupation numbers N_ℓ and c_ℓ are obtained by solving the coupled equations [Eqs. (7) and (8)]. Once they are determined, we can calculate the tunneling current by substituting Eq. (6) into Eq. (2). Figure 2 shows the tunneling current as a function of the applied bias at zero temperature and zero gate voltage. For simplicity, we have adopted the following energy and bias independent tunneling rates, $\Gamma_L=\Gamma_R=1$ meV. The tunneling current exhibits a staircaselike plateaus, arising from the well-known Coulomb blockade effect (including both intralevel and interlevel interactions). The length of each plateau indicates the energy level separation of adjacent resonant channels. The height of each step in the staircase indicates the probability strength of the resonant channel, which is determined by the one-electron and two-electron occupation numbers. To further analyze and resolve the current spectra, the differential conductance defined as dJ/dV_a is also plotted near the bottom in Fig. 2. The first eight peaks arising from the resonant channels are $\epsilon_1=E_1$, $\epsilon_2=E_1+U_1$, $\epsilon_3=E_2$, $\epsilon_4=E_1+U_1+U_{12}$, $\epsilon_5=E_2+U_2$, $\epsilon_6=E_2+U_{12}$, $\epsilon_7=E_1+U_1+2U_{12}$, and $\epsilon_8=E_2+U_2+U_{12}$. These differential conductance peaks have a Lorentzian shape of width $(\Gamma_L+\Gamma_R)/2$, which reveals the broadening of resonant channels. However, it is difficult to directly determine these important physical parameters by experiment because of the inhomogeneous broadening caused by other factors.

To examine the whole functionality of the SET, the tunneling current as a function of the gate voltage for various tunneling-rate ratios and at $V_a=10$ mV is plotted in Fig. 3. The tunneling current exhibits an oscillatory behavior, which is different from the staircase behavior shown in Fig. 2. Curves (a)–(e) correspond, respectively, $\Gamma_L=0.2$ meV, $\Gamma_L=0.4$ meV, $\Gamma_L=1$ meV, $\Gamma_L=5$ meV, and $\Gamma_L=10$ meV. Γ_R is fixed at 1 meV. In shell-tunneling condition $\Gamma_L/\Gamma_R<1$, the strengths of peaks arising from the E_1+U_1, $E_2+2U_{12}+U_2$, and $E_3+2U_{13}+2U_{23}+U_3$ are weaker than those of peaks arising from E_1, E_2+2U_{12}, and $E_3+2U_{13}+2U_{23}$. On the other hand, such a trend is oppositive in the shell-filling case, i.e., $\Gamma_L/\Gamma_R>1$. Many small satellite peaks are present. These peaks result from the fact that one-particle and two-particle occupation numbers have not yet reached one for the applied bias. For example, increasing Γ_L [going from (a) to (e)], the strengths of resonant channels E_2, $E_1+U_1+U_{12}$, and E_2+U_{12} are enhanced. It is worth noting that resonant channels resulting from the intralevel Coulomb interactions do not disappear even though $\Gamma_L/\Gamma_R\ll 1$. This is attributed to carriers blockaded by electrons in the right electrode, when the energy level of the quantum dot is tuned into continuum states below the Fermi energy of the right electrode. Note that the assumption of energy-independent tunneling rates is not very realistic since different orbitals have different coupling strengths to the band states of electrodes. In fact, one can measure the tunneling current spectra as functions of the gate voltage at small bias (V_a) and zero temperature to determine the different tunneling rates associated with different levels and reveal the orbital characteristics of CdSe QD if the widths of the peaks are larger than the inhomogeneous broadening caused by other factors.

Figure 4 shows a direct comparison of the calculated tunneling current spectrum with the measured one reported in Ref. 21, where the observed differential conductance peaks are broadened. To take into account the inhomogeneous broadening caused by either the Coulomb interactions from neighbor QDs or other factors, we replace each Lorentzian function appearing in the differential conductance by a Gaussian function of the form $f_i \exp\{-\frac{(\epsilon-\epsilon_i)^2}{2\rho_i^2}\}/(\rho_i\sqrt{2\pi})$. f_i, ϵ_i,

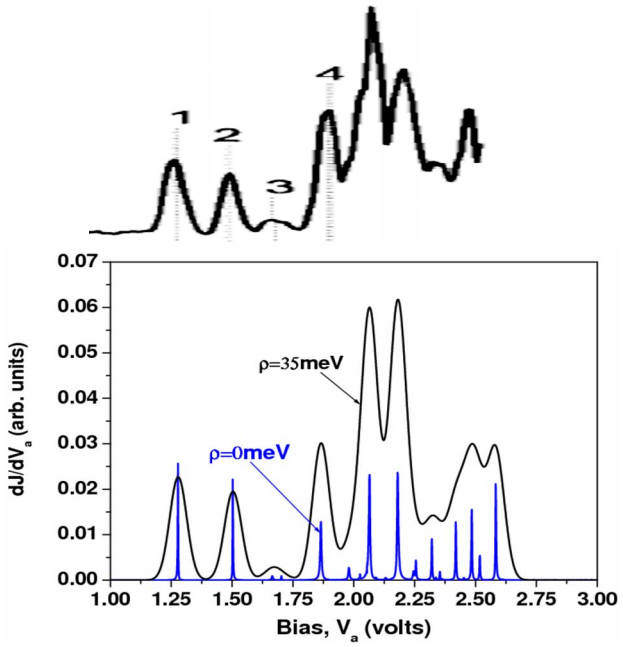

FIG. 4. (Color online) Differential conductance as functions of applied bias with and without the inhomogeneous broadening. For comparison, the experimental data taken from Ref. 21 is shown on top. Three one-particle energy levels for electrons in the QD are considered in the modeling.

and ρ_i denote the peak strength, resonance energy, and broadening width, respectively. The following parameters $\Gamma_{L,1}=1$ meV, $\Gamma_{R,1}=0.15$ meV, $\Gamma_{L,2}=3$ meV, $\Gamma_{R,2}=0.6$ meV, $\Gamma_{L,3}=1.5$ meV, and $\Gamma_{R,3}=0.375$ meV are adopted. The inhomogeneous broadening parameter is fixed at $\rho_i=35$ meV for all levels. As seen the figure, both the positions and relative strengths of these peaks are in very good agreement with the experimental measurement. Without the inhomogeneous broadening ($\rho=0$), the differential conductance spectrum exhibits many more sharp peaks, as shown in the lower part of the figure.

The proximity effect due to the coupling among multiple nanoparticles placed between two electrodes were reported in CdSe SETs.[21,22,36] Furthermore, negative differential conductance (NDC) due to the proximity effect has been observed for self-assembly Si quantum dots array. To describe the effect of interdot Coulomb interactions on the tunneling current, we consider the case of three weakly coupled quantum dots (dots A, B, and C). Dot A is placed at the center and dots B and C are placed at two sides of dot A. We consider a low bias situation, where only the ground states of the three QDs are involved. We assume the physical parameters of dot A are the same as those of the dot considered in Fig. 2. Dot B and dot C are identical dots with energy levels $E_B=E_C=E_A+20$ meV and intralevel Coulomb interaction $U_B=U_C=150$ meV. The interdot Coulomb interactions between dot B and dot C are disregarded due to the large interdot distance assumed. However, the interdot Coulomb interactions, U_{AB} and U_{AC}, are still appreciable and taken to be 30 meV. The parameters here fall into the regime $U_{\ell,j}>\Delta E=E_j-E_\ell$. We have shown that the two-particle occupation numbers play an important role in such a condition.[8] In Fig. 5, we plot the

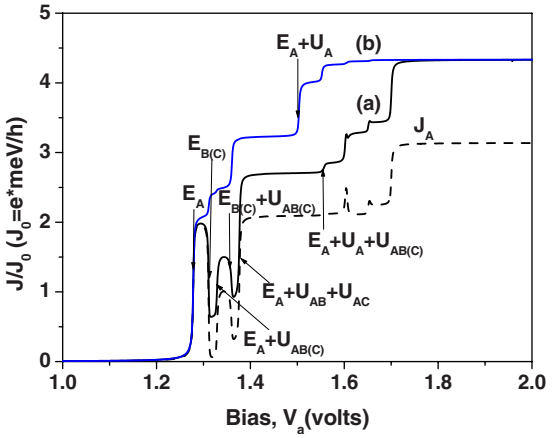

FIG. 5. (Color online) Tunneling current of a three QD junction as a function of the applied bias. In curve (a), dot B and dot C are in the shell-filling condition with $\Gamma_{B,L}=\Gamma_{C,L}=2$ meV and $\Gamma_{B,R}=\Gamma_{C,R}=0.1$ meV. The dashed curve is for the tunneling current through dot A alone (labeled J_A) under the same condition as in curve (a). In curve (b), dot B and dot C are in the shell-tunneling condition with $\Gamma_{B,L}=\Gamma_{C,L}=0.1$ meV and $\Gamma_{B,R}=\Gamma_{C,R}=2$ meV. The tunneling rates for dot A are $\Gamma_{A,L}=\Gamma_{A,R}=1$ meV in both cases.

tunneling current as a function of the applied bias for two case: (a) dot B and dot C are in the shell-filling condition and (b) dot B and dot C are in the shell-tunneling condition. Curve (a) exhibits NDC when dot B and dot C are in the shell-filling condition. Once dot B and dot C are in the shell-tunneling condition, as shown in curve (b), the NDC behavior disappears due to the suppression of interdot Coulomb interactions for small $N_B(N_C)$ and $N_{BB}(N_{CC})$. To clarify the origin of NDC, we plot the tunneling current through dot A alone J_A for the same condition as in curve (a), as the dashed curve in Fig. 5. Here, the tunneling currents through dot B and dot C are much smaller than J_A due to the small tunneling rates to the right lead. We focus on the case when the applied bias is insufficient to overcome the charging energy of any energy level. Then, the expression of $G^r_{A,\sigma}$ has the following simplified form:

$$G^r_{A,\sigma}(\epsilon)=(1-N_{A,-\sigma})\left[\frac{a_B a_C}{\mu_A}+\frac{a_B b_C}{\mu_A-U_{AC}}+\frac{b_B a_C}{\mu_A-U_{AB}}+\frac{b_B b_C}{\mu_A-U_{AB}-U_{AC}}\right], \quad (9)$$

where $\mu_A\equiv\epsilon-E_A+i(\Gamma_{A,L}+\Gamma_{A,R})/2$. In the beginning, the tunneling current J_A arises from electrons tunneling through the resonant channel E_A with probability $(1-N_{A,-\sigma})a_B a_C$. The probability factor $a_B a_C$ become reduced when some electrons tunnel through the energy levels of E_B and E_C. Consequently, J_A is suppressed. The tunneling current bounces back from the valley when more resonant channels E_A+U_{AB}, E_A+U_{AC}, and E_A are opened at higher bias. The decreasing of total probability of these three channels $(1-N_{A,-\sigma})(a_B+b_B a_C)$ once again suppress the tunneling current J_A when more electrons accumulate into dot B and dot C [note that carriers tunnel not only through channel $E_{B(C)}$ but also through channel $E_B+U_{AB}(E_C+U_{AC})$]. The tunneling

current resumes as the channel $E_A+U_{AB}+U_{AC}$ opens up when the bias further increases.

IV. BIPOLAR TUNNELING

So for, we have only discussed current generated by the electrons tunneling through resonant channels. Simultaneous electron and hole transport can occur and it has been observed in the negative bias regime.[21,22] In the system considered, the Fermi level (E_F) is much closer to the lowest conduction state than to the highest valence state [see Fig. 1(a)]. Therefore, a small forward bias can lead to the electron tunneling, while the holes remain blocked [see Fig. 1(b)]. On the other hand, a large reverse bias must be applied before the hole can tunnel into the quantum dot, which would also accompany the electron tunneling [see Fig. 1(c)]. Our formulas [Eqs. (4)–(8)] presented in Sec. II remain valid for such a situation, provided that the signs of particle energies and interlevel Coulomb energies are properly taken care of. For the holes, the energy levels are denoted by $E_{h,\ell}$, which are defined as the difference in energy of the lowest-lying conduction state and the corresponding valence state of concern. For the interlevel Coulomb energies, $U_{\ell,j}$ will be negative for two levels occupied by one electron and one hole and positive otherwise. Furthermore, the bipolar tunneling is accompanied by a radiative recombination. For the system considered in Ref. 21 under reverse bias, two-electron levels and two hole levels need to be involved. This correspond to a four-level system ($M=4$). For a hole tunneling through level $E_{h,\ell}$ while the other hole level j and electron levels 1 and 2 can be occupied by 0, 1, or 2 particles, the retarded Green's function is given by

$$G^r_{h\ell,\sigma}(\epsilon)=(\hat{a}_{hj}+\hat{b}_{hj}+c_{hj})(\hat{a}_{e2}+\hat{b}_{e2}+c_{e2})(\hat{a}_{e1}+\hat{b}_{e1}+c_{e1})\times\left\{\frac{1-N_{h\ell,-\sigma}}{\mu_{h,\ell}-2U_{hh,j\ell}+2U_{eh,1\ell}+2U_{eh,2\ell}}+\frac{N_{h\ell,-\sigma}}{\mu_{h,\ell}-U_{hh,\ell}-2U_{hh,j\ell}+2U_{eh,1\ell}+2U_{eh,2\ell}}\right\},\tag{10}$$

and similarly for an electron tunneling through level $E_{e\ell}$, we have

$$G^r_{e\ell,\sigma}(\epsilon)=(\hat{a}_{ej}+\hat{b}_{ej}+c_{ej})(\hat{a}_{h2}+\hat{b}_{h2}+c_{h2})(\hat{a}_{h1}+\hat{b}_{h1}+c_{h1})\times\left\{\frac{1-N_{e\ell,-\sigma}}{\mu_{e,\ell}-2U_{ee,j\ell}+2U_{eh,1\ell}+2U_{eh,2\ell}}+\frac{N_{e\ell,-\sigma}}{\mu_{e,\ell}-U_{ee,\ell}-2U_{eh,j\ell}+2U_{eh,1\ell}+2U_{eh,2\ell}}\right\},\tag{11}$$

where $\mu_{e(h),\ell}=\epsilon_{e(h),\ell}-E_{e(h),\ell}+i[\Gamma_{e(h),L,\ell}+\Gamma_{e(h),R,\ell}]/2$. $U_{ee,\ell}$ ($U_{hh,\ell}$) and $U_{eh,j\ell}$ denote the intralevel and interlevel electron (hole) Coulomb interactions, respectively. The signs preceding these Coulomb interactions are chosen such that all $U_{j,\ell}$'s are positive. Note that index $j\neq\ell$ in Eqs. (10) and (11) is restricted into the same band. $U_{eh,1\ell}$ and $U_{eh,2\ell}$ describe interband electron-hole Coulomb interactions. The above expressions are based on the assumption that $\Gamma_{e(h),\ell}\gg R_{e(h),\ell}$, where $\Gamma_{e(h)}$ and $R_{e(h),\ell}$ are the electron (hole) tunneling rates and electron-hole recombination rates involving level ℓ. The sum of electron and hole tunneling current in the reverse bias can be expressed as

$$J=\frac{-2e}{\hbar}\sum_\ell\left(\int\frac{d\epsilon_e}{2\pi}[f_{e,L}(\epsilon_e)-f_{e,R}(\epsilon_e)]T_e\ \mathrm{Im}\ G^r_{e,\ell,\sigma}(\epsilon_e)-\int\frac{d\epsilon_h}{2\pi}[f_{h,L}(\epsilon_h)-f_{h,R}(\epsilon_h)]T_h\ \mathrm{Im}\ G^r_{h,\ell,\sigma}(\epsilon_h)\right),\tag{12}$$

where $f_e(\epsilon)$ and $f_h(\epsilon)$ are the Fermi distribution functions for electrons and holes, respectively. $T_{e(h)}=\Gamma_{e(h),\ell,L}\Gamma_{e(h),\ell,R}/(\Gamma_{e(h),\ell,L}+\Gamma_{e(h),\ell,R})$. Note that we introduced the so-called hole electrodes in Eq. (12), which is empty states of electron electrodes. Let us consider the case where the energy gap of the quantum dot is $E_h+E_e=2.28$ eV.[21] Under the picture of hole electrodes, the ground state of holes will be 1.5 eV above the Fermi energy of hole electrodes. When the applied bias of left electron electrode is in the regime of negative bias, such a bias appears positive for holes in the left electrode. Because R_{eh} is typically less than 0.01 meV for semiconductor QDs (which is much smaller than the tunneling rates considered here), we can safely ignore the effect of radiative recombination on the average occupancy in the analysis here.

To describe the tunneling spectra observed in Refs. 21 and 22, some physical parameters relevant with holes and electron-hole Coulomb interactions should be determined. First, we adopt the energy level separation for holes as $E_{h,2}-E_{h,1}=80$ meV, which is much smaller than that between the ground state and the first excited state of electrons. The intralevel and interlevel hole Coulomb interactions are $U_{hh,11}=160$ meV, $U_{hh,22}=140$ meV, and $U_{hh,12}=U_{hh,21}=150$ meV. Due to the more localized wave function for holes (as a result of heavier effective mass for the valence band), it is expected that hole-hole Coulomb interactions are stronger than those for electrons. Meanwhile $U_{eh,11}=-130$ meV, $U_{eh,12}=-120$ meV, $U_{eh,21}=-108$ meV, and $U_{eh,22}=-85$ meV. The tunneling rates for electron and hole energy levels are given by $\Gamma_{e,1,L}=0.5$ meV, $\Gamma_{e,1,R}=0.1$ meV, $\Gamma_{e,2,L}=3.0$ meV, $\Gamma_{e,2,R}=0.6$ meV, $\Gamma_{h,1,L}=1.0$ meV, $\Gamma_{h,1,R}=0.6$ meV, $\Gamma_{h,2,L}=1.0$ meV, and $\Gamma_{h,2,R}=0.6$ meV. Figure 6 shows the calculated differential conductance as a function of the negative bias. Again, we take into account the inhomogeneous broadening effect by replacing each Lorentzian function appearing in the differential conductance by a Gaussian broadening function with width $\rho=35$ meV. For comparison, the experimental results taken from Ref. 21 are shown on the top of the figure. Our results for negative bias below −2.5 V agree well with the experiment. Because the experimental system is not stable in the strong negative bias regime, Jdira[21,22] did not show the tunneling spectra beyond −2.5 V. The complete spectra in the high bias regime (beyond −2.5 V) should involve more than four levels.

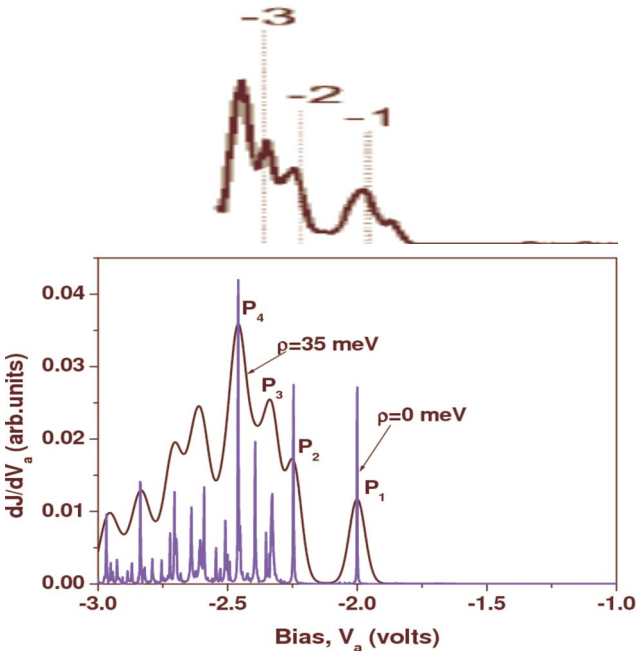

FIG. 6. (Color online) Differential conductance as a function of negative applied bias with and without the inhomogeneous broadening. For comparison, the experimental data taken from Ref. 21 is shown on top. Four one-particle energy levels in the QD (two for electrons and two for holes) are considered in the modeling.

According to the results shown in Fig. 6, the origin of each resonant channels can be clearly clarified. The first tunneling resonance corresponds to electrons of right electrode tunneling through $\epsilon_1=E_{e,1}$ level. Once electrons are injected into the quantum dot, holes in the left electrode are injected into the second resonant channel of $\epsilon_2=E_{h,1}-U_{eh,11}$. The broadened peaks P_1 and P_2 observed in Ref. 21 are attributed to these two resonant channels with more negative bias electrons tunnel through the third channel at $\epsilon_3=E_{e,2}-U_{eh,21}$. We also identify the subsequent resonant channels as $\epsilon_4=E_{e,1}+U_{ee,11}$, $\epsilon_5=E_{h,2}-U_{eh,12}$, $\epsilon_6=E_{e,2}-U_{eh,22}$, $\epsilon_7=E_{e,2}+U_{ee,12}-U_{eh,21}-U_{eh,22}$, $\epsilon_8=E_{e,2}+2U_{ee,12}-2U_{eh,21}-U_{eh,22}$, and $\epsilon_9=E_{h,1}$. Note that the corresponding voltages of ϵ_5 and ϵ_6 almost merge together. ϵ_8 and ϵ_9 are the same. Based on the tunneling rate ratios, electrons are in the shell-tunneling regime. On the other hand, holes are in the shell-filling regime. This indicates that holes tend to remain inside the QD during this bipolar tunneling process.

We also note that during the bipolar tunneling process, the electron and hole can recombine to produce a single-photon emission spectrum, which can be tuned by the applied bias. The electrically driven single-photon source has found important application in quantum communications.[37] Here we show that the bipolar tunneling process in an STM-tip/QD tunnel junction can produce interesting bias-dependent emission spectra of exciton complexes. For the sake of simplicity, only a two-level model is considered in the following study. We calculate the polarization for the spontaneous emission process and obtain the following form:

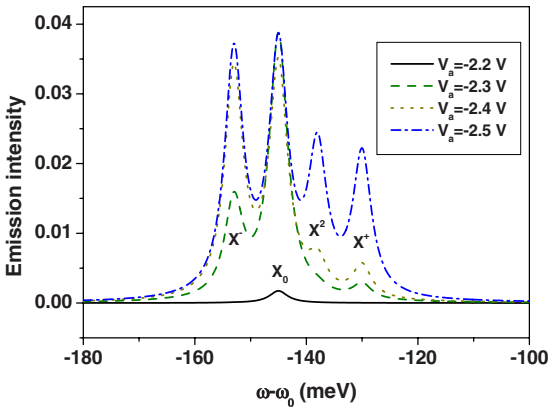

FIG. 7. (Color online) Emission spectra of exciton complexes for various applied biases in a reverse bias setup. $\omega_0=E_e+E_h$. X_0 denotes the exciton emission. X^- and X^+ denote the emission from negative trion and positive trion, respectively. X^2 denotes the biexciton emission.

$$P(\omega)=\lambda_{eh}^2\left(\frac{N_{X^0}}{\Omega_{X^0}}+\frac{N_{X^-}}{\Omega_{X^-}}+\frac{N_{X^+}}{\Omega_{X^+}}+\frac{N_{X^2}}{\Omega_{X^2}}\right). \tag{13}$$

where λ_{eh} is the Rabi frequency of an emission photon with angular frequency of ω. The emission spectrum strengths of exciton complexes are determined by the probability factors

$$N_{X^0}=N_{e,\sigma}N_{h,-\sigma}-\langle n_{e,-\sigma}n_{e,\sigma}\rangle N_{h,-\sigma}-\langle n_{h,-\sigma}n_{h,\sigma}\rangle N_{e,\sigma}+\langle n_{h,-\sigma}n_{h,\sigma}\rangle\langle n_{e,-\sigma}n_{e,\sigma}\rangle,$$

$$N_{X^-}=\langle n_{e,\sigma}n_{e,-\sigma}\rangle(N_{h,-\sigma}-\langle n_{h,\sigma}n_{h,-\sigma}\rangle)$$

$$N_{X^+}=\langle n_{h,\sigma}n_{h,-\sigma}\rangle(N_{e,\sigma}-\langle n_{e,\sigma}n_{e,-\sigma}\rangle),$$

and

$$N_{X^2}=\langle n_{h,\sigma}n_{h,-\sigma}\rangle\langle n_{e,\sigma}n_{e,-\sigma}\rangle,$$

which correspond, respectively, to the emission frequencies of exciton $\Omega_{X^0}=E_{e,1}+E_{h,1}-U_{eh,11}-\omega+i\Gamma$, negative trion $\Omega_{X^-}=E_{e,1}+E_{h,1}+U_{ee,11}-2U_{eh,11}-\omega+i\Gamma$, positive trion $\Omega_{X^+}=E_{e,1}+E_{h,1}+U_{hh,11}-2U_{eh,11}-\omega+i\Gamma$, and biexciton $\Omega_{X^2}=E_{e,1}+E_{h,1}+U_{hh,11}+U_{ee,11}-3U_{eh,11}-\omega+i\Gamma$.

In the absence of particle correlation, the polarization reduces to $P(\omega)=\lambda_{eh}^2N_eN_h/(E_{e,1}+E_{h,1}-\omega+i\Gamma)$. The imaginary part of $P(\omega)$ describes the emission spectra, which is shown in Fig. 7. Emission peaks due to the exciton, negative trion, positive trion, and biexciton are labeled by X^0, X^-, X^+, and X^2, respectively. Here we assume $U_h>U_{eh}>U_e$ since the hole tends to be more localized than the electron due to its heavier effective mass. Therefore, the biexciton emission peak (transition from the biexciton to the exciton) exhibits a blueshift from the exciton peak. Because the probability of each emission peak is determined by the occupation numbers, which are sensitive to the applied bias, it leads to dramatic changes in intensity for various peaks as the applied bias is varied. Such dramatic change was not observed in the *p-n* junction setup, as reported in Ref. 1, because the occupation number can be changed easily in that setup.

V. SUMMARY

A multiple-level Anderson model which takes into account the intralevel and interlevel Coulomb interactions is used to calculate the tunneling current spectra of quantum dot tunnel junctions. The tunneling current through the ground state and excited states of individual quantum dots are calculated in the framework of Green's function method. A closed form expression of the spectral function is derived and it provides a simple and efficient way to model the complicated tunneling current behavior of a quantum dot junction.

The tunneling current characteristics as functions of the applied bias V_a and gate voltage V_g are investigated. It is found that due to the Coulomb blockade effect, the tunneling-rate ratio can significantly influences the tunneling current spectra of the quantum dot junction. This indicates that the implementation of quantum dot junction should have precise control over the position, shape, and size of quantum dots in order to achieve the desired *IV* characteristics. We also point out that the negative differential conductance can be produced due to the interdot Coulomb interactions for a tunnel junction involving multiple QDs sandwiched between the metallic electrodes. Using a four-level model (two level for electrons and two level for holes), we can identify the origin of various peaks observed in the bipolar tunneling current spectra, as reported in Refs. 21 and 22. Finally, we show that the bipolar tunneling process can lead to a single-photon emission spectrum, which can be changed dramatically via the change in the applied bias.

ACKNOWLEDGMENTS

This work was supported by the National Science Council of the Republic of China under Contracts No. NSC 96-2221-E-008-108, 96-2120-M-008-001, and 95-2112-M-001-068-MY3.

APPENDIX A: QUANTUM DOT JUNCTION INVOLVING TWO LEVELS

In this appendix, we derive the retarded Green's function for the case with two levels. The derivations presented here will make the rigorous proof for the general case (as presented in Appendix B) much easier to follow. We consider a quantum dot with two levels denoted by ℓ and j $(j \neq \ell)$. From the equation of motion for $G^r_{\ell,\sigma}(t)$, we obtain

$$\mu_l G^r_{\ell,\sigma}(\epsilon) = 1 + U_\ell G^r_{\ell,\ell}(\epsilon) + U_{\ell,j}[G^r_{\ell,j,-\sigma}(\epsilon) + G^r_{\ell,j,\sigma}(\epsilon)], \tag{A1}$$

where $\mu_l \equiv \epsilon - E_\ell + i(\Gamma_{\ell,L}+\Gamma_{\ell,R})/2$ and $G^r_{\ell,\ell}(\epsilon) = \langle n_{\ell,-\sigma} d_{\ell,\sigma} d^\dagger_{\ell,\sigma}\rangle$, $G^r_{\ell,j,-\sigma}(\epsilon) = \langle n_{j,-\sigma} d_{\ell,\sigma} d^\dagger_{\ell,\sigma}\rangle$, and $G^r_{\ell,j,\sigma}(\epsilon) = \langle n_{j,\sigma} d_{\ell,\sigma} d^\dagger_{\ell,\sigma}\rangle$ are the two-particle Green's functions which are coupled to $G^r_{\ell,\sigma}$ via the intralevel and interlevel Coulomb interactions. $\Gamma_{\ell,L}$ and $\Gamma_{\ell,R}$ are the tunneling rates, describing the coupling between the quantum dot and the electrodes. Here, we have not included the effect of particle correlation on the tunneling rates. Such approximation is adequate for describing the Coulomb blockade, but not the Kondo effect.[9] In this paper, we only focus on the Coulomb blockade regime.

To solve Eq. (A1), we need to calculate the equation of motion of the two-particle Green's functions. They satisfy

$$(\mu_l - U_\ell) G^r_{\ell,\ell}(\epsilon) = N_{\ell,-\sigma} + U_{\ell,j}[G^r_{\ell,\ell,j,-\sigma}(\epsilon) + G^r_{\ell,\ell,j,\sigma}(\epsilon)], \tag{A2}$$

$$(\mu_l - U_{\ell,j}) G^r_{\ell,j,-\sigma}(\epsilon) = N_{j,-\sigma} + U_\ell G^r_{\ell,\ell,j,-\sigma}(\epsilon) + U_{\ell,j} G^r_{\ell,j,j}(\epsilon), \tag{A3}$$

and

$$(\mu_l - U_{\ell,j}) G^r_{\ell,j,\sigma}(\epsilon) = N_{j,\sigma} + U_\ell G^r_{\ell,\ell,j,\sigma}(\epsilon) + U_{\ell,j} G^r_{\ell,j,j}(\epsilon). \tag{A4}$$

$N_{\ell,-\sigma}$ and $N_{j,\sigma}$ $(N_{j,-\sigma})$ are the steady-state electron occupation numbers in the ℓth and jth level. Note that ℓ is not equal to j in Eqs. (A1)–(A4). Now the two-particle Green's functions are coupled to the following three-particle Green's functions: $G^r_{\ell,\ell,j,-\sigma}(\epsilon) = \langle n_{\ell,-\sigma} n_{j,-\sigma} d_{\ell,\sigma} d^\dagger_{\ell,\sigma}\rangle$, $G^r_{\ell,\ell,j,\sigma}(\epsilon) = \langle n_{\ell,-\sigma} n_{j,\sigma} d_{\ell,\sigma} d^\dagger_{\ell,\sigma}\rangle$, and $G^r_{\ell,j,j}(\epsilon) = \langle n_{j,-\sigma} n_{j,\sigma} d_{\ell,\sigma} d^\dagger_{\ell,\sigma}\rangle$. The equation of motion of the three-particle Green's functions will lead to coupling with the four-particle Green's functions, where the hierarchy terminates. Three particle Green's functions are given by

$$(\mu_l - U_\ell - U_{\ell,j}) G^r_{\ell,\ell,j,-\sigma}(\epsilon) = N_{\ell,-\sigma} N_{j,-\sigma} + U_{\ell,j} G^r_4, \tag{A5}$$

$$(\mu_l - U_\ell - U_{\ell,j}) G^r_{\ell,\ell,j,\sigma}(\epsilon) = N_{\ell,-\sigma} N_{j,\sigma} + U_{\ell,j} G^r_4, \tag{A6}$$

and

$$(\mu_l - 2U_{\ell,j}) G^r_{\ell,j,j}(\epsilon) = \langle n_{j,-\sigma} n_{j,\sigma}\rangle + U_\ell G^r_4, \tag{A7}$$

where $G^r_4 \equiv \langle n_{\ell,-\sigma} n_{j,-\sigma} n_{j,\sigma} d_{\ell,\sigma} d^\dagger_{\ell,\sigma}\rangle$ is the four-particle Green's function, which can be immediately solved since the hierarchy of equations of motion terminates here. We obtain

$$(\mu_l - U_\ell - 2U_{\ell,j}) G^r_4 = N_{\ell,-\sigma} \langle n_{j,-\sigma} n_{j,\sigma}\rangle. \tag{A8}$$

Consequently, these three-particle Green's functions can be expressed in the following closed form:

$$G^r_{\ell,\ell,j,-\sigma}(\epsilon) = N_{\ell,-\sigma}\left\{\frac{N_{j,-\sigma} - c_j}{\mu_l - U_\ell - U_{\ell,j}} + \frac{c_j}{\mu_l - U_\ell - 2U_{\ell,j}}\right\}, \tag{A9}$$

where $c_j \equiv \langle n_{j,-\sigma} n_{j,\sigma}\rangle$ denotes the two-particle occupation number in the same level j and we have used the identity

$$\frac{U_{\ell,j}}{(\mu_l - U_\ell - U_{\ell,j})(\mu_l - U_\ell - 2U_{\ell,j})} = \frac{1}{\mu_l - U_\ell - 2U_{\ell,j}} - \frac{1}{\mu_l - U_\ell - U_{\ell,j}}. \tag{A10}$$

Similarly,

$$G^r_{\ell,j,j}(\epsilon) = c_j\left\{\frac{1 - N_{\ell,-\sigma}}{\mu_l - 2U_{\ell,j}} + \frac{N_{\ell,-\sigma}}{\mu_l - U_\ell - 2U_{\ell,j}}\right\}. \tag{A11}$$

and

$$G^r_{\ell,\ell,j,\sigma}(\epsilon) + G^r_{\ell,\ell,j,-\sigma}(\epsilon) = N_{\ell,-\sigma}\left\{\frac{b_j}{\mu_l - U_\ell - U_{\ell,j}} + \frac{2c_j}{\mu_l - U_\ell - 2U_{\ell,j}}\right\}, \tag{A12}$$

where $b_j \equiv N_{j,-\sigma} + N_{j,\sigma} - 2c_j$ denotes the probability of finding one particle in the level j. Equation (A11) describes the mixed amplitudes for the propagation of an electron in level ℓ in the presence two other electrons in level j. Equation (A12) describes the mixed amplitudes for the propagation of n electron in level ℓ with another electron in the same level (with opposite spin) plus one more electron in level j (with either spin). From Eqs. (A9) and (A11), we observe a simple "sum rule:" the sum of the numerators of all terms (i.e., probability factors of all propagators) is always equal to the first term appearing in the right-hand side of the equation of motion for the Green's function, i.e., Eqs. (A5) and (A7). The probability factors for the remaining propagators are directly related to those appearing in the higher-particle-number Green's functions, which are coupled to the present one. This sum rule should always hold since all numerators are derived from partitions of the product of two fractions for the remaining terms. This sum rule will be very convenient for checking the derivations and it also allows easy determination of the probability factor of the leading propagator. Henceforth, for all the derivations below, we can determine the numerators for the nonleading terms first (which are easily obtained via partition of a product of two fractions) and then use the sum rule to determine the numerator of the leading term (which would be very tedious if we try to work out directly).

Substituting Eq. (A12) into Eq. (A2), we obtain

$$G^r_{\ell,\ell}(\epsilon) = N_{\ell,-\sigma}\left\{\frac{a_j}{\mu_l - U_\ell} + \frac{b_j}{\mu_l - U_\ell - U_{\ell,j}} + \frac{c_j}{\mu_l - U_\ell - 2U_{\ell,j}}\right\}, \tag{A13}$$

where $a_j \equiv 1 - b_j - c_j = 1 - N_{j,\sigma} - N_{j,-\sigma} + c_j$ is determined by using the sum rule and it denotes the probability of finding no particle in level j. Substituting Eqs. (A11) and (A12) into the sum of Eqs. (A3) and (A4), we obtain

$$G^r_{\ell,j,-\sigma}(\epsilon) + G^r_{\ell,j,\sigma}(\epsilon) = b_j\left[\frac{1 - N_{\ell,-\sigma}}{\mu_l - U_{\ell,j}} + \frac{N_{\ell,-\sigma}}{\mu_l - U_\ell - U_{\ell,j}}\right] + 2c_j\left[\frac{1 - N_{\ell,-\sigma}}{\mu_l - 2U_{\ell,j}} + \frac{N_{\ell,-\sigma}}{\mu_l - U_\ell - 2U_{\ell,j}}\right], \tag{A14}$$

where we have used the identity

$$\frac{(U_\ell + U_{\ell,j})2c_j N_{\ell,-\sigma}}{(\mu_l - U_{\ell,j})(\mu_l - U_\ell - 2U_{\ell,j})} = 2c_j N_{\ell,-\sigma}\left[\frac{1}{\mu_l - U_{\ell,j}} - \frac{1}{\mu_l - U_\ell - 2U_{\ell,j}}\right]. \tag{A15}$$

Note that the sum of the amplitudes of all propagators in Eq. (A14) is

$$b_j + 2c_j = N_{j,\sigma} + N_{j,-\sigma},$$

which again satisfies the sum rule mentioned above.

Inserting Eqs. (A13) and (A14) into Eq. (A1), we obtain the final expression

$$G^r_{\ell,\sigma}(\epsilon) = \sum_{k=1}^{3} p_k\left[\frac{(1 - N_{\ell,-\sigma})}{\mu_l - \Pi_k} + \frac{N_{\ell,-\sigma}}{\mu_l - U_\ell - \Pi_k}\right], \tag{A16}$$

where $\Pi_1 = 0, \Pi_2 = U_{\ell,j}$, and $\Pi_2 = 2U_{\ell,j}$. $p_1 = a_j$, $p_2 = b_j$, and $p_3 = c_j$. This result corresponds to Eq. (6) with $M = 2$.

According to the expression of the retarded Green's function of Eq. (6), we need to determine the average occupation numbers $N_{\ell,\sigma}(N_{\ell,-\sigma})$ and $N_{\ell,\ell}$, which can be calculated by $N_{\ell,\sigma} = \int (d\epsilon/2\pi i)\langle d_{\ell,\sigma} d^\dagger_{\ell,\sigma}\rangle^<$ and $N_{\ell,\ell} = \int (d\epsilon/2\pi i)\langle d_{\ell,\sigma} n_{\ell,-\sigma} d^\dagger_{\ell,\sigma}\rangle^<$, respectively.[38] The lesser Green's functions $\langle d_{\ell,\sigma} d^\dagger_{\ell,\sigma}\rangle^<$ and $\langle d_{\ell,\sigma} n_{\ell,-\sigma} d^\dagger_{\ell,\sigma}\rangle^<$ can be obtained by the equation of motion method[25,39] or the Dyson equation approach.[9] In the Coulomb blockade regime, we have $\langle d_{\ell,\sigma} d^\dagger_{\ell,\sigma}\rangle^< = 2f^<(\epsilon)\mathrm{Im}\, G^r_{\ell,\sigma}(\epsilon)$ and $\langle d_{\ell,\sigma} n_{\ell,-\sigma} d^\dagger_{\ell,\sigma}\rangle^< = 2f^<(\epsilon)\mathrm{Im}\, G^r_{\ell,\ell}(\epsilon)$, where $f^<(\epsilon) = -i[\Gamma_{\ell,L}(\epsilon) f_L(\epsilon) + \Gamma_{\ell,R} f_R(\epsilon)]/(\Gamma_{\ell,L} + \Gamma_{\ell,R})$. The above results lead to Eqs. (7) and (8), which can be used to calculate the average occupation numbers.

APPENDIX B: QUANTUM DOT JUNCTION WITH ARBITRARY NUMBER OF LEVELS

Now, we consider the general case with M levels ($M \geq 2$) labeled by $j = 1, \ldots, M$. Equations (A1) and (A2) become

$$\mu_l G^r_{\ell,\sigma}(\epsilon) = 1 + U_\ell G^r_{\ell,\ell}(\epsilon) + {\sum_j}' U_{\ell,j}[G^r_{\ell,j,-\sigma}(\epsilon) + G^r_{\ell,j,\sigma}(\epsilon)], \tag{B1}$$

where the prime on the summation means that the level ℓ is excluded.

$$(\mu_l - U_\ell) G^r_{\ell,\ell}(\epsilon) = N_{\ell,-\sigma} + {\sum_j}' U_{\ell,j}[G^r_{\ell,\ell,j,-\sigma}(\epsilon) + G^r_{\ell,\ell,j,\sigma}(\epsilon)]. \tag{B2}$$

We define the $(2+n)$- and $(1+n)$-particle ($n \leq 2M-2$) Green's functions as

$$G^r_{\ell,\ell,j_1,\ldots,j_n} = \langle n_{\ell,-\sigma} n_{j_1} \cdots n_{j_n} d_{\ell,\sigma} d^\dagger_{\ell,\sigma}\rangle,$$

and

$$G^r_{\ell,j_1,\ldots,j_n} = \langle n_{j_1} \cdots n_{j_n} d_{\ell,\sigma} d^\dagger_{\ell,\sigma}\rangle,$$

where $j_1, \ldots, j_n$ label any n states out of the $2(M-1)$ states (excluding spin up and down states in level ℓ). Here j_α is a

composite index for energy level and spin. In general, the $(2+n)$- and $(1+n)$-particle $(n \leq 2M-2)$ Green's functions satisfy

$$\left(\mu_l - U_\ell - \sum_{\alpha=1}^{n} U_{\ell,j_\alpha}\right) G^r_{\ell,\ell,j_1,\ldots,j_n} = N_{\ell,-\sigma}\langle n_{j_1}\cdots n_{j_n}\rangle + \sum_{j'}'' U_{\ell,j'} G^r_{\ell,\ell,j_1,\ldots,j_n,j'}, \quad \text{(B3)}$$

and

$$\left(\mu_l - \sum_{\alpha=1}^{n} U_{\ell,j_\alpha}\right) G^r_{\ell,j_1,\ldots,j_n} = \langle n_{j_1}\cdots n_{j_n}\rangle + U_\ell G^r_{\ell,\ell,j_1,\ldots,j_n} + \sum_{j'}'' U_{\ell,j'} G^r_{\ell,j_1,\ldots,j_n,j'}, \quad \text{(B4)}$$

where the "double prime" on the summation indicates that j' is not among the n states and not in the level ℓ. In the n-particle state labeled by $j_1,\ldots,j_n$, if there are m levels occupied with two particles and the rest singly occupied, we can label them by $j_1,j_1,\ldots,j_m,j_m,j_{2m+1},\ldots,j_n$. We then assume that the n-particle correlation function can be factorized as follows

$$\langle n_{j_1}\cdots n_{j_n}\rangle = c_{j_1}\cdots c_{j_m} N_{2m+1}\cdots N_n,$$

where $c_{j_i}=\langle n_{j_i} n_{j_i}\rangle$ denotes the two-particle correlation function in level j_i and $N_j=\langle n_j\rangle$ denotes the average occupancy in state j. Note that if we made the further approximation $c_{j_i} = N_{j_i} N_{j_i}$, it would then correspond to the Hartree–Fock approximation, typically adopted in the literature for studying the charge transport of an SET. Here, we shall go beyond the Hartree–Fock approximation by keeping the two-particle correlation functions when the two particles occupy the same level. They are evaluated by solving Eq. (8) self-consistently.

The $2M$-particle Green's function can be immediately solved since the hierarchy of equations of motion terminates there. We obtain

$$G^r_{2M} \equiv \left\langle n_{\ell,-\sigma} \prod_j{}' (n_{j,-\sigma} n_{j,\sigma}) d_{\ell,\sigma} d^\dagger_{\ell,\sigma} \right\rangle = \frac{N_{\ell,-\sigma} \prod_j{}' c_j}{\left(\mu_l - U_\ell - 2\sum_j{}' U_{\ell,j}\right)}, \quad \text{(B5)}$$

where Π'_j means taking the product of terms with subscript $j=1,\ldots,M$, excluding ℓ''. c_j is the probability of fining two particles in level j. The $(2M-1)$-particle Green's functions can then be solved by substituting Eq. (B5) into Eqs. (B3) and (B4). It is convenient to redefine the $(2M-m)$-particle Green's functions as

$$G^r_{\overline{j_1},\ldots,\overline{j_m}} \equiv G^r_{\ell,\ell,j_{m+1},\ldots,j_{2M-2}},$$

and

$$G^r_{\overline{\ell,-\sigma},\overline{j_1},\ldots,\overline{j_{m-1}}} \equiv G^r_{\ell,j_m,\ldots,j_{2M-m}},$$

where $\overline{j_1},\ldots,\overline{j_m}$ denotes states $\overline{1\cdots m}$ are unoccupied while all the rest are occupied and $\overline{\ell,-\sigma}$ denotes that the state $(\ell,-\sigma)$ is unoccupied. Following the same procedure as for deriving Eq. (A12), we obtain for the $(2M-1)$-particle Green's functions

$$\sum_{\sigma_1} G^r_{\overline{j_1,\sigma_1}} = N_{\ell,-\sigma}\left(\prod_j{}' c_j/c_{j_1}\right)\left\{\frac{b_{j_1}}{\mu_l - U_\ell - 2\sum_j{}' U_{\ell,j} + U_{\ell,j_1}} + \frac{2c_{j_1}}{\mu_l - U_\ell - 2\sum_j{}' U_{\ell,j}}\right\} \equiv (\hat{b}_{j_1} + 2c_{j_1}) G^r_{2M}/c_{j_1}, \quad \text{(B6)}$$

and

$$G^r_{\overline{\ell,-\sigma}} = \left(\prod_j{}' c_j\right)\left\{\frac{1-N_{\ell,-\sigma}}{\mu_l - 2\sum_j{}' U_{\ell,j}} + \frac{N_{\ell,-\sigma}}{\mu_l - U_\ell - 2\sum_j{}' U_{\ell,j}}\right\} \equiv (\hat{q}_\ell + 1) G^r_{2M}, \quad \text{(B7)}$$

where $\hat{q}_\ell \equiv N^{-1}_{\ell,-\sigma}\hat{b}_\ell$, and b_{j_1} denotes the probability of finding one particle in level j'_1 as defined previously. $\hat{b}_j$ $(\hat{b}_\ell)$ is an operator that puts a factor b_j $(b_\ell \equiv 1-N_{\ell,-\sigma})$ in the numerator and increases the value of the denominator by $U_{\ell,j}$ (U_ℓ) when acting on a fractional function.

To get the $(2M-2)$-particle Green's function, we substitute Eq. (B6) into Eq. (B3) and obtain [following the same procedure as for deriving Eq. (A13)]

$$G^r_{\overline{j_1 j_1}} = N_{\ell,-\sigma}\left(\prod_j{}' c_j/c_{j_1}\right)\left\{\frac{a_{j_1}}{\mu_l - U_\ell - 2\sum_j{}' U_{\ell,j} + 2U_{\ell,j_1}} + \frac{b_{j_1}}{\mu_l - U_\ell - 2\sum_j{}' U_{\ell,j} + U_{\ell,j_1}} + \frac{c_{j_1}}{\mu_l - U_\ell - 2\sum_j{}' U_{\ell,j}}\right\} \equiv (\hat{a}_{j_1} + \hat{b}_{j_1} + c_{j_1}) G^r_{2M}/c_{j_1}, \quad \text{(B8)}$$

where the two missing particles are associated with the same level j_1 and the spin indices of the pair have been omitted. $\hat{a}_j$ is an operator that puts a factor a_j in the numerator and increases the value of the denominator by $2U_{\ell,j}$ when acting on a propagator. When the two missing particles are associated with two different levels j_1 and j_2, we have

$$\sum_{\sigma_1\sigma_2} G^r_{\overline{j_1,\sigma_1},\overline{j_2,\sigma_2}} = N_{\ell,-\sigma}\left[\prod_j{}' c_j/(c_{j_1}c_{j_2})\right]\left\{\frac{b_{j_1}b_{j_2}}{\mu_l - U_\ell - 2\sum_j{}' U_{\ell,j} + U_{\ell,j_1} + U_{\ell,j_2}} + \frac{2b_{j_1}c_{j_2}}{\mu_l - U_\ell - 2\sum_j{}' U_{\ell,j} + U_{\ell,j_1}}\right.$$
$$\left. + \frac{2c_{j_1}b_{j_2}}{\mu_l - U_\ell - 2\sum_j{}' U_{\ell,j} + U_{\ell,j_2}} + \frac{4c_{j_1}c_{j_2}}{\mu_l - U_\ell - 2\sum_j{}' U_{\ell,j}}\right\}$$
$$= (\hat{b}_{j_1} + 2c_{j_1})(\hat{b}_{j_2} + 2c_{j_2})G^r_{2M}/(c_{j_1}c_{j_2}). \tag{B9}$$

Similarly, substitute Eqs. (B6) and (B7) into Eq. (B4) yields

$$\sum_{\sigma_1} G^r_{\overline{\ell,-\sigma},\overline{j_1,\sigma_1}} = \left(\prod_j{}' c_j/c_{j_1}\right)\left\{b_{j_1}\left[\frac{1 - N_{\ell,-\sigma}}{\mu_l - 2\sum_j{}' U_{\ell,j} + U_{\ell,j_1}} + \frac{N_{\ell,-\sigma}}{\mu_l - U_\ell - 2\sum_j{}' U_{\ell,j} + U_{\ell,j_1}}\right]\right.$$
$$\left. + 2c_{j_1}\left[\frac{1 - N_{\ell,-\sigma}}{\mu_l - 2\sum_j{}' U_{\ell,j}} + \frac{N_{\ell,-\sigma}}{\mu_l - U_\ell - 2\sum_j{}' U_{\ell,j}}\right]\right\}$$
$$= (\hat{q}_\ell + 1)(\hat{b}_{j_1} + 2c_{j_1})G^r_{2M}/c_{j_1}. \tag{B10}$$

To get the $(2M-3)$-particle Green's function, we substitute Eqs. (B8) and (B9) into Eq. (B3) and obtain

$$\sum_{\sigma_2} G^r_{\overline{j_1,j_1},\overline{j_2,-\sigma_2}} = N_{\ell,-\sigma}\left[\prod_j{}' c_j/(c_{j_1}c_{j_2})\right]\left\{\frac{a_{j_1}b_{j_2}}{\mu_l - U_\ell - 2\sum_j{}' U_{\ell,j} + 2U_{\ell,j_1} + U_{\ell,j_2}} + \frac{b_{j_1}b_{j_2}}{\mu_l - U_\ell - 2\sum_j{}' U_{\ell,j} + U_{\ell,j_1} + U_{\ell,j_2}}\right.$$
$$\left. + \frac{c_{j_1}b_{j_2}}{\mu_l - U_\ell - 2\sum_j{}' U_{\ell,j} + U_{\ell,j_2}} + \frac{2a_{j_1}c_{j_2}}{\mu_l - U_\ell - 2\sum_j{}' U_{\ell,j} + 2U_{\ell,j_1}} + \frac{2b_{j_1}c_{j_2}}{\mu_l - U_\ell - 2\sum_j{}' U_{\ell,j} + U_{\ell,j_1}} + \frac{2c_{j_1}c_{j_2}}{\mu_l - U_\ell - 2\sum_j{}' U_{\ell,j}}\right\}$$
$$= (\hat{a}_{j_1} + \hat{b}_{j_1} + c_{j_1})(\hat{b}_{j_2} + 2c_{j_2})G^r_{2M}/(c_{j_1}c_{j_2}), \tag{B11}$$

and

$$\sum_{\sigma_1\sigma_2\sigma_3} G^r_{\overline{j_1,\sigma_1},\overline{j_2,\sigma_2},\overline{j_3,\sigma_3}} = N_{\ell,-\sigma}\left[\prod_j{}' c_j/(c_{j_1}c_{j_2}c_{j_3})\right]\left\{\frac{b_{j_1}b_{j_2}b_{j_3}}{\mu_l - U_\ell - 2\sum_j{}' U_{\ell,j} + U_{\ell,j_1} + U_{\ell,j_2} + U_{\ell,j_3}} + \frac{2b_{j_1}b_{j_2}c_{j_3}}{\mu_l - U_\ell - 2\sum_j{}' U_{\ell,j} + U_{\ell,j_1} + U_{\ell,j_2}}\right.$$
$$+ \frac{2c_{j_1}b_{j_2}b_{j_3}}{\mu_l - U_\ell - 2\sum_j{}' U_{\ell,j} + U_{\ell,j_2} + U_{\ell,j_3}} + \frac{2b_{j_1}c_{j_2}b_{j_3}}{\mu_l - U_\ell - 2\sum_j{}' U_{\ell,j} + U_{\ell,j_1} + U_{\ell,j_3}} + \frac{4b_{j_1}c_{j_2}c_{j_3}}{\mu_l - U_\ell - 2\sum_j{}' U_{\ell,j} + U_{\ell,j_1}}$$
$$\left. + \frac{4c_{j_1}b_{j_2}c_{j_3}}{\mu_l - U_\ell - 2\sum_j{}' U_{\ell,j} + U_{\ell,j_2}} + \frac{4c_{j_1}c_{j_2}b_{j_3}}{\mu_l - U_\ell - 2\sum_j{}' U_{\ell,j} + U_{\ell,j_3}} + \frac{8c_{j_1}c_{j_2}c_{j_3}}{\mu_l - U_\ell - 2\sum_j{}' U_{\ell,j}}\right\}$$
$$= (\hat{b}_{j_1} + 2c_{j_1})(\hat{b}_{j_2} + 2c_{j_2})(\hat{b}_{j_3} + 2c_{j_3})G^r_{2M}/(c_{j_1}c_{j_2}c_{j_3}). \tag{B12}$$

Similarly, substituting Eqs. (B8)–(B10) into Eq. (B4) yields

$$G^r_{\overline{\ell,-\sigma},\overline{j_1 j_1}} = \left(\prod_j{}' c_j/c_{j_1}\right)\left\{a_{j_1}\left[\frac{1-N_{\ell,-\sigma}}{\mu_l - 2\sum_j{}' U_{\ell,j}} + \frac{N_{\ell,-\sigma}}{\mu_l - U_\ell - 2\sum_j{}' U_{\ell,j}}\right] + b_{j_1}\left[\frac{1-N_{\ell,-\sigma}}{\mu_l - 2\sum_j{}' U_{\ell,j} + U_{\ell,j_1}} + \frac{N_{\ell,-\sigma}}{\mu_l - U_\ell - 2\sum_j{}' U_{\ell,j} + U_{\ell,j_1}}\right] + c_{j_1}\left[\frac{1-N_{\ell,-\sigma}}{\mu_l - 2\sum_j{}' U_{\ell,j}} + \frac{N_{\ell,-\sigma}}{\mu_l - U_\ell - 2\sum_j{}' U_{\ell,j}}\right]\right\}$$

$$= (\hat{q}_\ell + 1)(\hat{a}_{j_1} + \hat{b}_{j_1} + c_{j_1})G^r_{2M}/c_{j_1}, \tag{B13}$$

and

$$\sum_{\sigma_1\sigma_2} G^r_{\overline{\ell,-\sigma},\overline{j_1,\sigma_1},\overline{j_2,\sigma_2}} = \left(\prod_j{}' c_j/c_{j_1}c_{j_2}\right)\left\{b_{j_1}b_{j_2}\left[\frac{1-N_{\ell,-\sigma}}{\mu_l - 2\sum_j{}' U_{\ell,j} + U_{\ell,j_1} + U_{\ell,j_2}} + \frac{N_{\ell,-\sigma}}{\mu_l - U_\ell - 2\sum_j{}' U_{\ell,j} + U_{\ell,j_1} + U_{\ell,j_2}}\right] + 2b_{j_1}c_{j_2}\left[\frac{1-N_{\ell,-\sigma}}{\mu_l - 2\sum_j{}' U_{\ell,j} + U_{\ell,j_1}} + \frac{N_{\ell,-\sigma}}{\mu_l - U_\ell - 2\sum_j{}' U_{\ell,j} + U_{\ell,j_1}}\right] + 2c_{j_1}b_{j_2}\left[\frac{1-N_{\ell,-\sigma}}{\mu_l - 2\sum_j{}' U_{\ell,j} + U_{\ell,j_2}} + \frac{N_{\ell,-\sigma}}{\mu_l - U_\ell - 2\sum_j{}' U_{\ell,j} + U_{\ell,j_2}}\right] + 4c_{j_1}c_{j_2}\left[\frac{1-N_{\ell,-\sigma}}{\mu_l - 2\sum_j{}' U_{\ell,j}} + \frac{N_{\ell,-\sigma}}{\mu_l - U_\ell - 2\sum_j{}' U_{\ell,j}}\right]\right\}$$

$$= (\hat{q}_\ell + 1)(\hat{b}_{j_1} + 2c_{j_1})(\hat{b}_{j_2} + 2c_{j_2})G^r_{2M}/(c_{j_1}c_{j_2}). \tag{B14}$$

Based on the above derivations, we can now prove the following two theorems.

Theorem 1. The $(2+n)$-particle Green's functions for m singly occupied levels and $(n'-m)$ empty levels [with any choice of n' and m subject to the constraints $n' \le M$, $0 < m < n'$, and $2(M-n')+m=2+n$] satisfy the following relation:

$$\sum_{\sigma_1,\ldots,\sigma_m} G^r_{\overline{j_1\sigma_1,\ldots,j_m\sigma_m},\overline{j_{m+1}j_{m+1},\ldots,j_{n'}j_{n'}}} = \left[\prod_{i=1}^{m}(\hat{b}_{j_i} + 2c_{j_i})\prod_{i=m+1}^{n'}(\hat{a}_{j_i} + \hat{b}_{j_i} + c_{j_i})\right]G^r_{2M}\Big/\prod_{i=1}^{n'} c_i$$

$$= \prod_{k=1}^{2^m\times 3^{n'-m}} \frac{p_k}{\mu_\ell - U_\ell - \Pi_k}, \tag{B15}$$

where levels $j_1,\ldots,j_m$ are singly occupied, levels $j_{m+1},\ldots,j_{n'}$ are empty, and the remaining $(M-n')$ levels are doubly occupied. Each term in the sum represents a "propagator" with probability p_k given by the product of the corresponding coefficients and the pole occurring at the corresponding energy Π_k, which is determined by counting the occupancies of levels associated with the configuration.

Theorem 2. The $(1+n)$-particle Green's functions for $m+1$ singly occupied levels (including the level ℓ) and $(n'-m)$ empty levels [with any choice of n' and m subject to the constraints $n' \le M$, $0 < m < n'$, and $2(M-n')+m=2+n$] satisfy the following relation:

$$\sum_{\sigma_1,\ldots,\sigma_m} G^r_{\overline{\ell,-\sigma},\overline{j_1\sigma_1,\ldots,j_m\sigma_m},\overline{j_{m+1}j_{m+1},\ldots,j_{n'}j_{n'}}} = (\hat{q}_\ell + 1)\prod_{i=1}^{m}(\hat{b}_{j_i} + 2c_{j_i})\prod_{i=m+1}^{n'}(\hat{a}_{j_i} + \hat{b}_{j_i} + c_{j_i})G^r_{2M}\Big/\prod_{i=1}^{n'} c_{j_i}$$

$$= \sum_{i}^{2^m\times 3^{n'-m}}\left[\frac{q_\ell p_k}{\mu_\ell - \Pi_k} + \frac{p_k}{\mu_\ell - U_\ell - \Pi_k}\right]. \tag{B16}$$

The above two theorems can be proved via induction. We already shown from Eqs. (B6)–(B14) that Theorem 1 is valid for the cases $2+n \ge 2M-3$ and Theorem 2 is valid for the cases $1+n \ge 2M-3$. Assuming that case n is valid if we can show that Case $(n-1)$ is also valid, then the above two theorems are proved. Let us consider a $(2+n-1)$-particle Green's function, which is obtained by removing one particle from the $(2+n)$-particle Green's function as described in Theorem 1. Assume that the particle is removed from the level j_r, which can be any level other than $j_{m+1},\ldots,j_{n'}$ or ℓ. There are two possible situations: (a) j_r does not coincide with one of the levels in $j_1,\ldots,j_m$ and (b) j_r coincides with one of the levels in $j_1,\ldots,j_m$. We first consider

the situation (a). Substituting Eq. (B15) into Eq. (B3) and summing over all spin indices for singly occupied levels yields

$$\begin{aligned}
&\sum_{\sigma_r,\sigma_1,\ldots,\sigma_m} G^r_{\overline{j_r\sigma_r,j_1\sigma_1,\ldots,j_m\sigma_m},\overline{j_{m+1}j_{m+1},\cdots,j_{n'}j_{n'}}} \\
&= \left(\mu_l - U_\ell - 2\sum_j{}' U_{\ell,j} + \prod_{i=1}^{m} U_{\ell,j_i} + 2\sum_{i=m+1}^{n'} U_{\ell,j_i} + U_{\ell,j_r}\right)^{-1} \\
&\quad \times \left\{ N_{\ell,-\sigma} \sum_{\sigma_r,\sigma_1,\ldots,\sigma_m} \langle n_{j_r\sigma_r} n_{j_1\sigma_1} \cdots n_{j_m\sigma_m}\rangle \prod_{i=n'+1}^{M} c_i + \sum_{\sigma_r}\sum_{j'}{}' U_{\ell,j'} \hat{P}_{j',j_r\sigma_r} \prod_{i=1}^{m} (\hat{b}_{j_i} + 2c_{j_i}) \prod_{i=m+1}^{n'} (\hat{a}_{j_i} + \hat{b}_{j_i} + c_{j_i}) G^r_{2M} \Big/ \prod_{i=1}^{n'} c_i \right\} \\
&= \left(\mu_l - U_\ell - 2\sum_j{}' U_{\ell,j} + \sum_{i=1}^{m} U_{\ell,j_i} + 2\sum_{i=m+1}^{n'} U_{\ell,j_i} + U_{\ell,j_r}\right)^{-1} \\
&\quad \times \left\{ N_{\ell,-\sigma}(N_{j_r,+} + N_{j_r,-}) \prod_{i=1}^{m} (N_{j_i,+} + N_{j_i,-}) \prod_{i=n'+1}^{M} c_i + \sum_{\sigma_r}\sum_{j'}{}'' U_{\ell,j'} \hat{P}_{j',j_r\sigma_r} \sum_{k=1}^{2^m\times 3^{n'-m}} \frac{p_k}{\mu_\ell - U_\ell - \Pi_k} \right\},
\end{aligned} \tag{B17}$$

where $\hat{P}_{j',j_r\sigma_r}$ is a permutation operator that replaces the index j' with $j_r\sigma_r$. j' is a composite index for spin and orbital that runs through all the states, which are not occupied in the $(2+n-1)$ configuration. There are $n_r=2M-n-1$ states available. The permutation operator affects all the coefficients in the term that follows (i.e., p_k and Π_k). When $j'=j_r\sigma_r$, the $(2+n-1)$-particle configuration considered here is coupled to the $(2+n)$-particle configuration, as described in Eq. (B15). When $j'\neq j_r\sigma_r$, it converts an operator $\hat{b}_{j'}$ to $\hat{b}_{j_r}$ or an operator $\hat{a}_{j'}$ to $\hat{b}_{j_r}\hat{b}_{j'}$, thus changing the probability factor p_k and the pole Π_k. For a permutation with j' labeling a singly occupied level, we obtain $2^m\times 3^{n'-m}$ propagators, while for j' labeling an empty level, we obtain $2^{m+2}\times 3^{n'-m-1}$ propagators. We can prove that

$$\begin{aligned}
\sum_{\sigma_r,\sigma_1,\ldots,\sigma_m} G^r_{\overline{j_r\sigma_r,j_1\sigma_1,\ldots,j_m\sigma_m},\overline{j_{m+1}j_{m+1},\cdots,j_{n'}j_{n'}}} &= (\hat{b}_{j_r} + 2c_{j_r}) \prod_{i=1}^{m} (\hat{b}_{j_i} + 2c_{j_i}) \prod_{i=m+1}^{n'} (\hat{a}_{j_i} + \hat{b}_{j_i} + c_{j_i}) G^r_{2M} \Big/ \left[c_{j_r} \prod_{i=1}^{n'} c_{j_i} \right] \\
&= \prod_{k=1}^{2^{(m+1)}\times 3^{n'-m}} \frac{p'_k}{\mu_\ell - U_\ell - \Pi'_k},
\end{aligned} \tag{B18}$$

which takes the same form as Eq. (B15). To see this, we first show that for every propagator appearing in Eq. (B18), there is a corresponding propagator in Eq. (B17) with the same denominator. It is easy to see that the first term (the leading propagator) in Eq. (B17) has the same denominator as the term $[\hat{b}_{j_r}(\Pi_{i=1}^{m}\hat{b}_{j_i})(\Pi_{i=m+1}^{n'}\hat{a}_{j_i})]G^r_{2M}$ in Eq. (B18), which represents a configuration of $(2+n-1)$ particles. For all the other terms, which represent configurations with $(2+n)$ or more particles, we can always find it from the product $[\Pi_{i=1}^{m}(\hat{b}_{j_i}+2c_{j_i})\Pi_{i=m+1}^{n'}(\hat{a}_{j_i}+\hat{b}_{j_i}+c_{j_i})]G^r_{2M}$ via suitable permutation of indices. For example, the term

$$\hat{b}_{j_r}\left[\left(\prod_{i=1}^{m-2}\hat{b}_{j_i}\right)c_{j_{m-1}}c_{j_m}\left(\prod_{i=m+1}^{n'}\hat{a}_{j_i}\right)\right]G^r_{2M}$$

appearing in Eq. (B18) can be obtained via the permutation $\hat{P}_{j_{m-1},j_r}$ or $\hat{P}_{j_m,j_r}$ in Eq. (B17). Likewise, the term

$$\hat{b}_{j_r}\left[\left(\prod_{i=1}^{m}\hat{b}_{j_i}\right)\hat{b}_{j_{m+1}}\left(\prod_{i=m+2}^{n'}\hat{a}_{j_i}\right)\right]G^r_{2M}$$

can be obtained via the permutation $\hat{P}_{j_{m+1},j_r}$. For any given term in this group, the numerator obtained from Eq. (B17) (not including the factor $U_{\ell,j'}$) is always the same as that from Eq. (B18), since it only involves a permutation of states and the numerator always equal to the corresponding probability factor p_k for that configuration.

Next, we show that a given term in Eq. (B18), which corresponds to a $(2+n-1+n'')$-particle configuration (where n'' is an integer between 1 and $2M-n-1$) can always be matched by making a permutation from the product $[\Pi_{i=1}^{m}(\hat{b}_{j_i}+2c_{j_i})\Pi_{i=m+1}^{n'}(\hat{a}_{j_i}+\hat{b}_{j_i}+c_{j_i})]G^r_{2M}$ with n'' different ways. For the start, it is easy to see that the term $c_{j_r}(\Pi_{i=1}^{m}2c_{j_i})(\Pi_{i=m+1}^{n'}c_{j_i})G^r_{2M}/[c_{j_r}\Pi_{i=1}^{n'}c_{j_i}]$ in Eq. (B18) can be matched by applying any of the $n_r=2M-1-n$ permutations

on the product $(\Pi_{i=1}^{m}2c_{j_i})(\Pi_{i=m+1}^{n'}c_{j_i})G_{2M}^{r}/\Pi_{i=1}^{n'}c_{j_i}$ in Eq. (B17) since the c operators are just plain numbers, and they have no effect on the denominator of the term. For the analysis below, we are not concerned with the numerator of the term. Thus, the presence of an $\hat{a}_j$ operator will be treated as the product of two $\hat{b}$ operators, $\hat{b}_{j+}\hat{b}_{j-}$ (the + and − indicate the two spin states). When a $\hat{b}_{j_a}$ operator appears in a given product of Eq. (B18), the permutation $P_{j',j_r\sigma_r}$ with $j'=j_a$ must be excluded since we cannot replace $\hat{b}_{j_a}$ by $\hat{b}_{j_r}$ and produce a match. Thus, for the $(2+n-1+n'')$-particle configuration in Eq. (B17), there are (n_r-n'') $\hat{b}$ operators, $\hat{b}_{j_1},\ldots,\hat{b}_{j_{n_r-n''}}$ appear in the product, and we must exclude the permutations with $j'=j_1,\ldots,\hat{j}_{n_r-n''}$ and left with n'' different permutations.

Therefore, we have shown that

$$\sum_{\sigma_r}\sum_{j'}{}''U_{\ell,j'}\hat{P}_{j',j_r\sigma_r}\sum_{k}^{2^m\times 3^{n'-m}}\frac{p_k}{\mu_\ell-U_\ell-\Pi_k}=\sum_{k=2}^{2^{m+1}\times 3^{n'-m}}\left(\sum_{i=1}^{n''(k)}U_{\ell,j_i'}\right)\frac{p_k'}{\mu_\ell-U_\ell-\Pi_k'}. \tag{B19}$$

Namely, every term labeled k in Eq. (B18) is matched from the sum of n'' terms (n'' depends on k) in Eq. (B17) except the leading term ($k=1$). Furthermore, the prefactor for this term $\Sigma_{i=1}^{n''}\hat{U}_{\ell,j_i'}$ must be equal to the difference in energy denominator between the term and the leading propagator. This is obvious since the leading term is produced by the product $\hat{b}_{j_1},\ldots,\hat{b}_{j_{n_r}}$ and the term of concern is produced by the product $\hat{b}_{j_1},\ldots,\hat{b}_{j_{n_r-n''}}$. Thus, such a term can always be written as

$$\left(\mu_l-U_\ell-2\sum_{j}{}'U_{\ell,j}+\sum_{i=1}^{m}U_{\ell,j_i}+2\sum_{i=m+1}^{n'}U_{\ell,j_i}+U_{\ell,j_r}\right)^{-1}\left(\sum_{j'=1}^{n''}\hat{U}_{\ell,j'}\right)\frac{p_k'}{\mu_\ell-U_\ell-\Pi_k'}$$
$$=\frac{p_k'}{\mu_\ell-U_\ell-\Pi_k'}-\frac{p_k'}{\mu_l-U_\ell-2\sum_j{}'U_{\ell,j}+\sum_{i=1}^{m}U_{\ell,j_i}+2\sum_{i=m+1}^{n'}U_{\ell,j_i}}. \tag{B20}$$

So it introduces a coefficient $-p_k'$ to the numerator of the leading propagator. Thus, the numerator of the leading propagator becomes

$$N_{\ell,-\sigma}(N_{j_r,+}+N_{j_r,-})\prod_{i=1}^{m}(N_{j_i,+}+N_{j_i,-})\prod_{i=n'+1}^{M}c_i-\sum_{k=2}^{2^{(m+1)}\times 3^{n'-m}}p_k',$$

which can be shown to be the same as p_1' in Eq. (B18). Namely, the sum rule described above is satisfied. This is verified via the relation

$$\sum_k p_k'\Bigg/\left(\prod_{i=n'+1}^{M}c_i\right)=N_{\ell,-\sigma}(b_{j_r}+2c_{j_r})\left[\prod_{i=1}^{m}(b_{j_i}+2c_{j_i})\prod_{i=m+1}^{n'}(a_{j_i}+b_{j_i}+c_{j_i})\right]$$
$$=N_{\ell,-\sigma}(N_{j_r,+}+N_{j_r,-})\prod_{i=1}^{m}(N_{j_i,+}+N_{j_i,-}), \tag{B21}$$

since $a_{j_i}+b_{j_i}+c_{j_i}=1$ and $b_{j_i}+2c_{j_i}=N_{j_i,+}+N_{j_i,-}$. Therefore, we have proved that if Eq. (B15) is valid for a $(2+n)$-particle configuration with m singly occupied levels and $(n'-m)$ empty levels, the same equation holds for a $(2+n-1)$-particle configuration with $m+1$ singly occupied levels and $(n'-m)$ empty levels.

Next, we consider the situation (b) when we remove one particle from the level j_r, where j_r coincides with one of the levels in $j_1\cdots j_m$. Without losing generality, we let $j_r=j_m$. Namely, we want to prove that

$$\sum_{\sigma_1,\ldots,\sigma_{m-1}}G^{r}_{\overline{j_1\sigma_1,\ldots,j_{m-1}\sigma_{m-1}},\overline{j_mj_m,j_{m+1}j_{m+1},\ldots,j_{n'}j_{n'}}}=\prod_{i=1}^{m-1}(\hat{b}_{j_i}+2c_{j_i})\prod_{i=m}^{n'}(\hat{a}_{j_i}+\hat{b}_{j_i}+c_{j_i})G_{2M}^{r}\Bigg/\left[\prod_{i=1}^{n'}c_{j_i}\right] \tag{B22}$$

is valid, provided that Theorem 1 is valid. However, since Theorem 1 is valid for any choice of configuration subject to the constraints. We can write a equation similar to Eq. (B15) for the following $(2+n)$-particle Green's function:

$$\sum_{\sigma_1,\ldots,\sigma_{m-2}}G^{r}_{\overline{j_1\sigma_1,\ldots,j_{m-2}\sigma_{m-2}},\overline{j_rj_r,j_mj_m,\ldots,j_{n'}j_{n'}}},$$

which is for the configuration with $(m-2)$ singly occupied levels and $(n'+1-m)$ empty levels. Since Eq. (B22) also describes the situation where one particle is removed from level j_m-1 (which does not coincide with one of the levels $j_1,\ldots,j_{m-2}$ from

the configuration described above, we can use the relation just proved for situation (a) as described by Eq. (B18) to prove that Eq. (B22) is valid. Consequently, Theorem 1 is valid for any $(2+n-1)$-particle Green's function provided that it holds for any $(2+n)$-particle Green's function.

To prove Theorem 2, we consider a $(1+n-1)$-particle configuration, in which the levels ℓ, j_r, and $j_1,\ldots,j_m$ are singly occupied, $j_{m+1},\ldots,j_{n'}$ are empty, and the rest of the M levels are doubly occupied. Here we only consider the situation where j_r does not coincide with one of the levels in $j_1,\ldots,j_m$ [i.e., situation (a) as discussed above for proving Theorem 1]. Substituting Eqs. (B15) and (B16) into Eq. (B4) for this configuration yields

$$\begin{aligned}
&\sum_{\sigma_r,\sigma_1,\cdots,\sigma_m} G^r_{\ell,-\sigma,\overline{j_r\sigma_r,j_1\sigma_1,\ldots,j_m\sigma_m,j_{m+1}j_{m+1},\ldots,j_{n'}j_{n'}}} \\
&= \left(\mu_l - 2\sum\nolimits_j U_{\ell,j} + \sum_{i=1}^{m} U_{\ell,j_i} + 2\sum_{i=m+1}^{n'} U_{\ell,j_i} + U_{\ell,j_r}\right)^{-1} \Bigg\{ N_{\ell,-\sigma} \sum_{\sigma_r,\sigma_1,\ldots,\sigma_m} \langle n_{j_r\sigma_r} n_{j_1\sigma_1}\cdots n_{j_m\sigma_m}\rangle \prod_{i=n'+1}^{M} c_i \\
&\quad + U_\ell \left[(\hat{b}_{j_r} + 2c_{j_r}) \prod_{j=1}^{m} (\hat{b}_j + 2c_j) \prod_{i=m+1}^{n'} (\hat{a}_i + \hat{b}_i + c_i) \right] G^r_{2M} \Big/ \prod_{i=1}^{n'} c_i + (\hat{q}_\ell + 1) \sum_{\sigma_r} \sum\nolimits_{j'} U_{\ell,j'} \hat{P}_{j',j_r\sigma_r} \\
&\quad \times \left[\prod_{j=1}^{m} (\hat{b}_j + 2c_j) \prod_{i=m+1}^{n'} (\hat{a}_i + \hat{b}_i + c_i) \right] G^r_{2M} \Big/ \prod_{i=1}^{n'} c_i \Bigg\} \\
&= \left(\mu_l - 2\sum\nolimits_j U_{\ell,j} + \sum_{i=1}^{m} U_{\ell,j_i} + 2\sum_{i=m+1}^{n'} U_{\ell,j_i} + U_{\ell,j_r}\right)^{-1} \Bigg\{ (N_{j_r,+} + N_{j_r,-}) \prod_{i=1}^{m} (N_{j_i,+} + N_{j_i,-}) \prod_{i=n'+1}^{M} c_i \\
&\quad + 2U_\ell \sum_{k=1}^{2^{m+1}\times 3^{n'-m}} \frac{p'_k}{\mu_\ell - U_\ell - \Pi'_k} + (\hat{q}_\ell + 1) \sum_{\sigma_r} \sum\nolimits_{j'} U_{\ell,j'} \hat{P}_{j',j_r\sigma_r} \sum_{k}^{2^m\times 3^{n'-m}} \frac{p_k}{\mu_\ell - U_\ell - \Pi_k} \Bigg\},
\end{aligned} \tag{B23}$$

where $\hat{P}_{j',j_r}$ is a permutation operator that replaces the index j' with $j_r\sigma_r$. j' runs through all the states (including spin) that are not occupied in the $(1+n-1)$ configuration, excluding the level ℓ. $(j'=1,\ldots,n_r;\ n_r \equiv 2M-n-1)$ Substituting Eq. (B19) into Eq. (B23), we obtain

$$\begin{aligned}
&\sum_{\sigma_r,\sigma_1,\ldots,\sigma_m} G^r_{\ell,-\sigma,\overline{j_r\sigma_r,j_1\sigma_1,\ldots,j_m\sigma_m,j_{m+1}j_{m+1},\ldots,j_{n'}j_{n'}}} \\
&= \left(\mu_l - 2\sum\nolimits_j U_{\ell,j} + \sum_{i=1}^{m} U_{\ell,j_i} + 2\sum_{i=m+1}^{n'} U_{\ell,j_i} + U_{\ell,j_r}\right)^{-1} \Bigg\{ (N_{j_r,+} + N_{j_r,-}) \prod_{i=1}^{m} (N_{j_i,+} + N_{j_i,-}) \prod_{i=n'+1}^{M} c_i \\
&\quad + U_\ell \left[\sum_{k=1}^{2^{m+1}\times 3^{n'-m}} \frac{p'_k}{\mu_\ell - U_\ell - \Pi'_k} \right] + (\hat{q}_\ell + 1) \left[\sum_{k=2}^{2^{m+1}\times 3^{n'-m}} \left(\sum_{i=1}^{n''(k)} U_{\ell,j'_i} \right) \frac{p'_k}{\mu_\ell - U_\ell - \Pi'_k} \right] \Bigg\} \\
&= \left(\mu_l - 2\sum\nolimits_j U_{\ell,j} + \sum_{i=1}^{m} U_{\ell,j_i} + 2\sum_{i=m+1}^{n'} U_{\ell,j_i} + U_{\ell,j_r}\right)^{-1} \Bigg\{ (N_{j_r,+} + N_{j_r,-}) \prod_{i=1}^{m} (N_{j_i,+} + N_{j_i,-}) \prod_{i=n'+1}^{M} c_i \\
&\quad + U_\ell \frac{p'_1}{\mu_\ell - U_\ell - \Pi'_1} + \sum_{k=2}^{2^{m+1}\times 3^{n'-m}} \left[\left(\sum_{i=1}^{n''(k)} U_{\ell,j'_i} \right) \frac{q_\ell p'_k}{\mu_\ell - \Pi'_k} + \left(U_\ell + \sum_{i=1}^{n''(k)} U_{\ell,j'_i} \right) \frac{p'_k}{\mu_\ell - U_\ell - \Pi'_k} \right] \Bigg\}.
\end{aligned} \tag{B24}$$

Using the partition of product of fractions, we obtain

$$\sum\nolimits_{\sigma_r,\sigma_1,\ldots,\sigma_m} G^r_{\overline{j_r\sigma_r,j_1\sigma_1,\ldots,j_m\sigma_m,j_{m+1}j_{m+1},\ldots,j_{n'}j_{n'}}} = (\hat{q}_\ell + 1)(\hat{b}_{j_r} + 2c_{j_r}) \left[\prod_{i=1}^{m} (\hat{b}_{j_i} + 2c_{j_i}) \prod_{i=m+1}^{n'} (\hat{a}_{j_i} + \hat{b}_{j_i} + c_{j_i}) \right] \cdot$$

$$G^r_{2M} \Big/ \left[c_{j_r} \prod_{i=1}^{n'} c_{j_i} \right] = \sum_{k=1}^{2^{(m+1)}\times 3^{n'-m}} \left[\frac{q_\ell p'_k}{\mu_\ell - \Pi'_k} + \frac{p'_k}{\mu_\ell - U_\ell - \Pi'_k} \right],$$

which takes the same form as Eq. (B16). The sum rule can also be easily verified since

$$\sum_k (q_\ell + 1)p'_k = N^{-1}_{\ell,-\sigma} \sum_k p'_k = (N_{j_r,+} + N_{j_r,-}) \prod_{i=1}^{m} (N_{j_i,+} + N_{j_i,-}) + U_\ell \frac{p'_1}{\mu_\ell - U_\ell - \Pi'_1}.$$

The situation (b) (i.e., when j_r coincides with one of the levels in $j_1 \cdots j_m$) can be similarly proved by adopting the same argument as in proving Theorem 1. Therefore, Theorem 2 is also proved. Using Theorems 1 and 2 and take the limit $n=0$ ($m=0$ and $n'=M-1$), we immediately obtain the final expression for the two-particle and one-particle Green's functions as given in Eqs. (5) and (6).

*ychang15@uiuc.edu
†mtkuo@ee.ncu.edu.tw

[1] Z. L. Yuan, B. E. Kardynal, R. M. Stevenson, A. J. Shield, C. J. Lobo, K. Cooper, N. S. Beattlie, D. A. Ritchie, and M. Pepper, Science **295**, 102 (2002).
[2] David M.-T. Kuo and Y. C. Chang, Phys. Rev. B **72**, 085334 (2005).
[3] L. Zhuang, L. Guo, and S. Y. Chou, Appl. Phys. Lett. **72**, 1205 (1998).
[4] M. Saitoh, N. Takahashi, H. Ishikuro, and T. Hiramoto, Jpn. J. Appl. Phys., Part 1 **40**, 2010 (2001).
[5] C. Macchivavello, G. M. Palma, and A. Zeilingger, *Quantum Computation and Quantum Information Theory* (World Scientific, Singapore, 1999).
[6] D. Fologea, M. Gershow, B. Ledden, D. S. McNabb, J. A. Golovchenko, and J. L. Li, Nano Lett. **5**, 1905 (2005).
[7] A. S. Alexandrov, A. M. Bratkovsky, and R. S. Williams, Phys. Rev. B **67**, 075301 (2003).
[8] David M.-T. Kuo and Y. C. Chang, Phys. Rev. Lett. **99**, 086803 (2007).
[9] H. Haug and A. P. Jauho, *Quantum Kinetics in Transport and Optics of Semiconductors* (Springer, Heidelberg, 1996).
[10] Y. M. Niquet, G. Allan, C. Delerue, and M. Lannoo, Appl. Phys. Lett. **77**, 1182 (2000).
[11] A. Franceschetti, H. Fu, L. W. Wang, and A. Zunger, Phys. Rev. B **60**, 1819 (1999).
[12] O. Stier, M. Grundmann, and D. Bimberg, Phys. Rev. B **59**, 5688 (1999).
[13] S. J. Sun and Y. C. Chang, Phys. Rev. B **62**, 13631 (2000).
[14] C. C. Kaun and T. Seideman, Phys. Rev. Lett. **94**, 226801 (2005).
[15] Y. C. Chen, M. Zwolak, and M. Di Ventra, Nano Lett. **4**, 1709 (2004).
[16] U. Banin, Y. Cao, D. Katz, and O. Millo, Nature (London) **400**, 542 (1999).
[17] O. Millo, D. Katz, Y. W. Cao, and U. Banin, Phys. Rev. Lett. **86**, 5751 (2001).
[18] E. P. A. M. Bakkers, Z. Hens, A. Zunger, A. Franceschetti, L. P. Kouwenhoven, L. Gurevich, and D. Vanmaekelbergh, Nano Lett. **1**, 551 (2001).
[19] Y. M. Niquet, C. Delerue, G. Allan, and M. Lannoo, Phys. Rev. B **65**, 165334 (2002).
[20] S. W. Wu, G. V. Nazin, X. Chen, X. H. Qiu, and W. Ho, Phys. Rev. Lett. **93**, 236802 (2004).
[21] L. Jdira, P. Liljeroth, E. Stoffels, D. Vanmaekelbergh, and, S. Speller, Phys. Rev. B **73**, 115305 (2006).
[22] P. Liljeroth, L. Jdira, K. Overgaag, B. Grandidier, S. Speller, and D. Vanmaekelbergh, Phys. Chem. Chem. Phys. **8**, 3845 (2006).
[23] L. V. Keldysh, Zh. Eksp. Teor. Fiz. **47**, 1515 (1964); [Sov. Phys. JETP **20** 1018 (1965)].
[24] A. P. Jauho, N. S. Wingreen, and Y. Meir, Phys. Rev. B **50**, 5528 (1994).
[25] R. Swirkowicz, J. Barnas, and M. Wilczynski, Phys. Rev. B **68**, 195318 (2003).
[26] D. Pfannkuche and S. E. Ulloa, Phys. Rev. Lett. **74**, 1194 (1995).
[27] Y. Meir and N. S. Wingreen, Phys. Rev. Lett. **68**, 2512 (1992).
[28] Q. F. Sun and H. Guo, Phys. Rev. B **66**, 155308 (2002).
[29] David M.-T. Kuo and Y. C. Chang, Phys. Rev. B **61**, 11051 (2000).
[30] Y. Meir, N. S. Wingreen, and P. A. Lee, Phys. Rev. Lett. **66**, 3048 (1991).
[31] Y. Meir, N. S. Wingreen, and P. A. Lee, Phys. Rev. Lett. **70**, 2601 (1993).
[32] C. W. J. Beenakker, Phys. Rev. B **44**, 1646 (1991).
[33] W. C. W. Chan and S. M. Nie, Science **281**, 2016 (1998).
[34] G. P. Mitchell, C. A. Mirkin, and R. L. Letsinger, J. Am. Chem. Soc. **121**, 8122 (1999).
[35] D. L. Klein, R. Roth, A. K. L. Lim, A. P. Alivisatos, and P. L. McEuen, Nature (London) **389**, 699 (1997).
[36] L. W. Yu, K. J. Chen, J. Song, J. M. Wang, J. Xu, W. Li, and X. F. Huang, Thin Solid Films **515**, 5466 (2007).
[37] A. Imamoglu and Y. Yamamoto, Phys. Rev. Lett. **72**, 210 (1994).
[38] B. R. Bulka and T. Kostyrko, Phys. Rev. B **70**, 205333 (2004).
[39] C. Niu, D. L. Lin, and T. H. Lin, J. Phys.: Condens. Matter **11**, 1511 (1999).